SFSWAP is a negative regulator of OGT intron detention and global pre-mRNA splicing

Ashwin Govindan[1] and Nicholas K. Conrad[1]*

[1]Department of Microbiology

University of Texas Southwestern Medical Center

Dallas, TX 75390

Running title: SFSWAP regulates OGT intron detention

*Corresponding author: Nicholas.Conrad@utsouthwestern.edu

Abstract

O-GlcNAcylation is the reversible post-translational addition of β-N-acetylglucosamine to serine and threonine residues of nuclear and cytoplasmic proteins. It plays an important role in several cellular processes through the modification of thousands of protein substrates. O-GlcNAcylation in humans is mediated by a single essential enzyme, O-GlcNAc transferase (OGT). OGT, together with the sole O-GlcNAcase OGA, form an intricate feedback loop to maintain O-GlcNAc homeostasis in response to changes in cellular O-GlcNAc using a dynamic mechanism involving nuclear retention of its fourth intron. However, the molecular mechanism of this dynamic regulation remains unclear. Using an O-GlcNAc responsive GFP reporter cell line, we identify SFSWAP, a poorly characterized splicing factor, as a trans-acting factor regulating OGT intron detention. We show that SFSWAP is a global regulator of retained intron splicing and exon skipping that primarily acts as a negative regulator of splicing. In contrast, knockdown of SFSWAP leads to reduced inclusion of a ‘decoy exon’ present in the OGT retained intron which may mediate its role in OGT intron detention. Global analysis of decoy exon inclusion in SFSWAP and UPF1 double knockdown cells indicate altered patterns of decoy exon usage. Together, these data indicate a role for SFSWAP as a global negative regulator of pre-mRNA splicing and positive regulator of intron retention.

Introduction

Intron retention (IR) refers to the lack of removal of specific introns in a transcript, resulting in full-length introns in an RNA (1, 2). IR that leads to impaired cytoplasmic export and nuclear retention of the transcript is referred to as intron detention (3). Detained introns are a common feature of mammalian transcriptomes, but, unlike other forms of alternate splicing, intron detention controls the levels and timing of production of mature mRNA (3-5). Cells regulate the efficiency of splicing of DIs, and therefore mRNA production, in response to specific environmental cues. DI-containing transcripts may serve as nuclear reservoirs that are spliced in response to cellular environment, or they may be transcriptional dead-ends that are subjected to nuclear degradation pathways (3, 5-8). Intron detention regulates a wide variety of transcripts in mammals, but the environmental cues and mechanisms that regulate intron detention have been defined for only a few of these RNAs.

The environmental cues that regulate intron detention of the human O-linked β-N-acetylglucosamine (O-GlcNAc) transferase (OGT) protein have been defined, but the mechanisms of this regulation are not fully understood (9). OGT encodes the sole enzyme responsible for the post-translational modification O-GlcNAc, where UDP-GlcNAc serves as the cofactor for addition of GlcNAc residues to the hydroxyl groups of serine and threonine residues of thousands of nuclear and cytoplasmic proteins (10-13). Conversely, OGA (O-GlcNAcase) is the sole enzyme responsible for removal of O-GlcNAc (14). Cells maintain O-GlcNAc homeostasis by an intricate feedback mechanism involving intron detention of the OGT transcript (9). Under conditions of high cellular O-GlcNAc (such as treatment with the OGA inhibitor thiamet G [TG]), intron 4 of OGT is detained, resulting in reduction in cytoplasmic OGT mRNA. However, under conditions of low cellular O-GlcNAc (such as glucose deprivation or treatment with the OGT inhibitor OSMI-1), the intron is rapidly excised, resulting in increased levels of cytoplasmic OGT mRNA. Interestingly, the OGA transcript is also regulated by intron detention, but with the inverse relationship to O-GlcNAc levels outcomes as OGT (15).

We previously identified a cis-acting intronic splicing silencer (ISS) situated within OGT intron 4 that is necessary for intron retention (9). Subsequent work by other groups

showed that the ISS overlaps with an ~150 bp unannotated ‘decoy exon’ possessing multiple weak 5´ and 3´ splice sites (16). Deletion of the OGT decoy exon/ISS or even blocking of the decoy 5´ splice sites using morpholino oligonucleotides renders splicing of intron 4 constitutive (9, 17). This suggests the somewhat counterintuitive idea that at least partial assembly of the spliceosome around the decoy is necessary for OGT intron detention even though splicing of the decoy exon does not occur. Decoy exons are not unique to OGT and are present in many other retained intron containing genes, specifically those with longer retained introns (16, 18). The decoy exons mediate intron retention in these genes as well, but the precise mechanism by which decoy exons regulate intron retention remains unclear.

In addition to the role of OGT intron detention in buffering changes in cellular O-GlcNAc levels, OGT (and consequently O-GlcNAc) has been proposed to be a ‘master regulator’ of detained intron splicing (15). Treatment of cells with the OGT inhibitor OSMI-2 for short time periods (~30 min) induces changes in OGT detention to buffer O-GlcNAc levels. However, longer treatment durations (~2 h) lead to global changes in detained intron splicing. Differential phosphoproteomics after a short OSMI-2 treatment identified a set of proteins enriched in splicing factors. These ‘early responders’ could potentially mediate downstream effects of OSMI-2 on splicing and included the putative splicing factor SFSWAP.

SFSWAP (splicing factor, suppressor of white-apricot homolog; SFRS8) encodes the essential human homolog of the drosophila splicing factor SWAP (19). It is an alternate splicing factor containing an RS domain, but it does not possess a canonical RNA binding domain (19). It contains two suppressor of white apricot/Prp21 (SURP) domains which mediate its binding to other proteins containing a SURP interaction domain. The second SURP domain of SFSWAP has been shown to interact with the mammalian branchpoint binding protein SF1 *in vitro* (20). However, the identity of its regulatory targets remains unknown. Its sequence contains a number of known phosphorylation sites (15) indicating that its function might be regulated by phosphorylation. In addition, it regulates alternate splicing of Tau (21), CD45 and fibronectin (22) by inhibiting the inclusion of specific exons.

Here, we identify SFSWAP as a regulator of OGT intron detention using a CRISPR knockout screen with an O-GlcNAc responsive GFP reporter cell line. We show that knockout of SFSWAP leads to enhanced splicing of the OGT detained intron, particularly under high-O-GlcNAc conditions, indicating its role as a negative regulator of OGT splicing. We also show that SFSWAP is a global regulator of detained intron splicing and exon skipping, with enhanced splicing of retained introns and increased inclusion of cassette exons upon SFSWAP knockdown. Our results suggest that SFSWAP regulates OGT intron detention by modulating the inclusion or recognition of the decoy exon present within the detained intron. Finally, global analysis of decoy exon splicing upon SFSWAP knockdown indicates that SFSWAP may regulate decoy exon splicing globally to mediate its effect on intron detention.

Results

A GFP splicing reporter that monitors cellular O-GlcNAc levels

To enable genetic screens for identification of trans-acting factors that regulate OGT intron detention, we constructed a GFP-based splicing reporter that responds to cellular O-GlcNAc levels. The reporter consists of the entire intron 4 of OGT (the detained intron) and corresponding exons (exons 4 and 5) flanked upstream and downstream by the efficiently spliced β-globin intron 2 (and corresponding exons 2 and 3) (Fig. 1a) (23). An eGFP reporter upstream of this assembly is driven by a constitutive CMV promoter and translationally separated from the remaining exons by a T2A element (24). The T2A element induces ribosomal skipping (25) producing a GFP polypeptide separate from the protein product of the β-globin-OGT exons.

We integrated this reporter into the AAVS1 safe harbor locus of HCT116 cells by TALEN-mediated recombination and isolated clonal cell lines harboring the reporter (26). Treatment of cells with the OGA inhibitor TG induces high O-GlcNAc levels. This should promote detention of OGT intron 4, nuclear retention of the transcript, and reduced expression of the GFP reporter. On the other hand, treatment with OGT inhibitor OSMI-1 induces a low O-GlcNAc condition, which should promote intron 4

splicing, cytoplasmic export of the mRNA, and increased GFP expression (Fig 1a, right). RT-PCR analysis of reporter RNA from clonal cell lines yielded a predominant single band corresponding to the mature reporter mRNA indicating the absence of unexpected splicing events (Fig. 1b). Moreover, this band increased and decreased upon OSMI-1 and TG treatment, as expected. Further screening of reporter lines by northern blot analysis also confirmed that the GFP reporter is responsive to cellular O-GlcNAc levels. Treatment of the reporter line with 1 μM TG for 6 h led to reduced levels of the spliced product, while treatment with 10 μM OSMI-1 for the same time led to enhanced splicing increased levels of the reporter mRNA (Fig. 1c). FACS analysis of the reporter lines treated with the inhibitors verified GFP protein expression, with lower and higher GFP fluorescence after TG and OSMI-1 treatment, respectively (Fig. 1d). To further characterize reporter activity at various O-GlcNAc levels, we treated reporter clones with conditions known to perturb cellular O-GlcNAc levels. Treatment of the reporter cells with glucosamine or the OGA inhibitor PUGNAc (O-(2-Acetamido-2-deoxy-D-glucopyranosylidene)amino N-phenyl carbamate) resulted in reduced GFP protein levels similar to TG, while treatment with the GFAT inhibitor DON (6-diazo-5-oxo-L-norleucine) or glucose deprivation led to increased GFP levels (Fig. 1e). Finally, we validated the reporter line by knockdown of OGT itself, which will reduce cellular O-GlcNAc levels. As expected, we observed increased levels of reporter mRNA upon OGT knockdown (Fig. 1f). Together, these results demonstrate that our GFP reporter construct reflects the response of endogenous OGT to intracellular O-GlcNAc levels.

SFSWAP is a negative regulator of OGT intron 4 splicing

To screen for trans-acting factors that regulate OGT intron retention, we performed whole genome CRISPR knockout screens using the Brunello knockout library (27) under 3 treatment conditions – TG, OSMI-1 or untreated. Treatment of reporter lines with TG brings the cells to a ‘low GFP’ state under which knockout of negative splicing regulatory factors (i.e., those promoting intron retention) are expected to result in a ‘high GFP’ state. Treatment with OSMI-1 results in cells that are ‘high GFP’ and knockout of factors that promote splicing of the retained intron will result in a ‘low GFP’ state. Finally,

untreated cells can be selected for either 'low GFP' or 'high GFP' events. We performed pilot screens at 100X library coverage with a 10-day knockout time period and 24 h treatment with inhibitors just before selection for either 'high' or 'low GFP' cells by FACS sorting. Subsequent sequencing of the guide RNA locus from the sorted cells and statistical analysis using MAGeCK (28) identified candidates to regulate OGT intron retention. While we did not obtain any hits with the OSMI-1 and untreated 'low GFP' screens, we successfully obtained hits with both the TG and untreated 'high GFP' screens. Since the list of putative targets from both screens were comparable (Suppl. Fig. S1), we performed 2 additional replicates of the screen at 300X coverage under TG treatment conditions only and obtained similar results.

As expected, the top hit from the screens was OGT itself (Fig. 2a). In addition, we obtained many hits corresponding to genes involved in glucose metabolism including GFAT (Fig. 1e) and SLC2A1 (a glucose transporter), further boosting our confidence that the genes identified in the screen are relevant to O-GlcNAc homeostasis. We also obtained a few hits corresponding to RNA binding proteins (e.g., HNRNPU, HuR) and proteins involved in m6A modification (ZC3H13, KIAA1429). Interestingly, the large majority of the hits were splicing associated factors and/or components of the spliceosome. The latter was surprising because loss of core spliceosome factors would be expected to result in reduced splicing of the reporter (and thus low GFP levels), but we selected for 'high GFP' cells. Nevertheless, these results indicated that the hits from the screen may be associated with a specific spliceosome-mediated mechanism.

We next validated some of the top hits by siRNA mediated knockdown and northern blot analysis or RT-qPCR for the spliced and retained intron junctions of the endogenous OGT transcript (Suppl. Fig. S2). Consistently, knockdown of SFSWAP increased GFP expression (Fig. 2b) and enhanced splicing of the reporter RNA (Fig. 2c, left). To check whether SFSWAP knockdown also results in splicing changes in endogenous OGT, we performed northern blot analysis with a probe corresponding to the 3´ UTR of OGT mRNA. Knockdown of SFSWAP in these cells under TG treatment conditions resulted in enhanced splicing of the retained intron compared to the non-target control (Fig. 2c, right) indicating that the action of SFSWAP was not limited to the reporter. To accurately

quantify the changes in splicing in OGT upon SFSWAP knockdown, we performed RT-qPCR on OGT RNA isolated from either non-target or SFSWAP knockdown cells under various conditions (Fig. 2d). Knockdown of SFSWAP resulted in a significant increase in the spliced form of OGT RNA compared to non-target both under DMSO (~1.8 fold) and TG-treated conditions (~3 fold). Knockdown in OSMI-1 treatment conditions did not result in a further increase in spliced RNA levels. Together, these data suggest that SFSWAP is a negative regulator of OGT intron 4 splicing.

SFSWAP is a global regulator of detained intron and skipped exon splicing

Despite its similarity to splicing factors, the importance of SFSWAP in human gene expression and splicing remains unclear. To characterize the functional role of SFSWAP, we performed RNA-seq in either non-target (siNT) or SFSWAP knockdown (siSFSWAP) cells in the absence of TG or OSMI-1. Differential expression analysis using edgeR revealed 252 downregulated and 633 upregulated genes on SFSWAP knockdown, but did not reveal any functional class of RNAs that was regulated by SFSWAP. Since SFSWAP is a predicted splicing factor, we performed alternate splicing analysis using the rMATS package (29). We analyzed five alternate splicing event types – retained introns (RI), skipped exons (SE), alternate 5´ splice sites (A5SS), alternate 3´ splice sites (A3SS) and mutually exclusive exons (MXE). Interestingly, we found global changes in splicing patterns between siNT and siSFSWAP, with the majority of changes occurring across two of the five event types analyzed – retained introns and skipped exons (Fig. 3a). To visualize this more clearly, we plotted the inclusion level differences between the two conditions (IncLevelDifference, calculated as $IncLevel_{siNT}$ - $IncLevel_{siSFSWAP}$) against FDR values obtained from rMATS. A positive value for IncLevelDifference indicates more removal of retained introns in SFSWAP knockdown compared to siNT, while a negative value indicates more retention. Knockdown of SFSWAP resulted in increased excision of retained introns globally, indicated by more events with a positive value for IncLevelDiffference (Fig. 3b) and as exemplified by genome browser shots of IFRD2 and GFUS/TSTA3 (Fig. 3c) This is consistent with the original screen phenotype, where SFSWAP was isolated as negative regulator of OGT

retained intron splicing (Fig. 2). Previous observations that SFSWAP autoregulates its own expression by control of splicing of its first two retained introns is also consistent with this observation (30, 31). Taken together, these data support the conclusion that SFSWAP promotes intron retention of a wide variety of transcripts.

In the case of skipped exon events, a positive value for IncLevelDifference indicates increased skipping (reduced inclusion) of the exon upon SFSWAP knockdown, while a negative value indicates increased inclusion. We observed a general enhancement of skipped exon inclusion upon SFSWAP knockdown (Fig. 3b). This is in agreement with previous studies where SFSWAP was shown to promote exclusion of CD45 exon 4 and the IICS region of fibronectin (22). Our results are also consistent with the observation that SFSWAP inhibits inclusion of Tau exon 10 (21). For increased rigor, we also performed alternate splicing analysis using two other pipelines, MAJIQ (32) and Whippet (33). Although the number of differential splicing events identified by these pipelines were lower than with rMATS, the trends remained similar (Suppl. Fig. S3 and S4). These results are consistent with a role for SFSWAP in splicing regulation and further suggest a more prominent role as a negative regulator of splicing.

To obtain further insights into the targets of SFSWAP, we looked at the sequence features of these SFSWAP-dependent differentially regulated splice events including length, GC content and splice site strength. While we did not find any significant differences among the events with respect to length or splice site strength, we observed some interesting trends with respect to GC content. In RIs that are more efficiently spliced upon SFSWAP knockdown (positive IncLevelDifference), we found that the average GC content in the RI and flanking exons was higher compared to those that less efficiently spliced (Fig. 3d). We observed similar trends toward higher GC content when we examined skipped exon events that result in enhanced inclusion upon SFSWAP knockdown (negative IncLevelDifference). In this case, the skipped exon, upstream and downstream exons all had higher GC content. Together these results suggest that SFSWAP is a global regulator of pre-mRNA splicing that primarily regulates intron retention and exon skipping events.

SFSWAP regulates OGT decoy exon inclusion

To delineate the mechanism of SFSWAP regulation of OGT intron retention, we further looked into our RNA-seq dataset. Interestingly, genome browser visualization revealed no obvious changes in sequence coverage at the OGT retained intron locus after SFSWAP knockdown (Suppl. Fig. S5). Although surprising, this agrees with the RT-qPCR results on the retained intron junction upon SFSWAP knockdown (Fig. 2d), where we saw no statistically significant changes in RI junction usage. We reasoned that the lack of junction usage changes could be because the RNA-seq was performed under untreated conditions, while both the CRISPR screen and confirmatory RT-qPCRs were performed under TG-treated conditions (Fig. 2, S2). To test whether the effect of SFSWAP knockdown on the OGT retained intron is more appreciable under TG-treated conditions, we repeated the RNA-seq analysis after 6 h of TG treatment. Visualization of OGT detained intron splicing under these conditions using a sashimi plot provided support for enhanced removal of the detained intron upon SFSWAP knockdown (Suppl. Fig. S6). Alternate splicing analysis using this dataset reproduced previous results that SFSWAP is a global regulator of pre-mRNA splicing. The effect of SFSWAP on global intron retention was, if anything, stronger under TG treatment conditions (Suppl. Fig. S7).

Recognition of the decoy exon within the OGT retained intron plays an important part in regulation of intron retention in OGT (9, 16). Since one of the phenotypes of SFSWAP knockdown is a change in skipped exon splicing, and the decoy mimics a skipped exon internal to the RI, we wanted to test if decoy exon inclusion levels were altered upon SFSWAP knockdown. To do this, we performed RT-qPCR analysis under UPF1 knockdown conditions in the presence of TG to stabilize the decoy exon form, which otherwise would be subject to nonsense-mediated decay (NMD). Under these conditions, we saw reduced inclusion of the decoy exon upon SFSWAP knockdown (Fig. 4a). We also performed semi-quantitative RT-PCR followed by nanopore sequencing of the region between exon 3 and exon 8 of OGT mRNA to obtain a comprehensive picture of splicing in the region. Consistent with the RT-qPCR analysis,

there was a ~5 fold reduction in sequencing reads containing the decoy exon upon SFSWAP knockdown (Fig. 4b).

To further test the role SFSWAP on OGT decoy exon splicing, we analyzed changes in decoy exon inclusion in the TG treated RNA-seq dataset. The decoy exon in OGT has two predicted 5´ splice sites and 2 predicted 3´ splice sites. To quantify changes in decoy exon inclusion, we mapped the RNA-seq reads to a version of the human genome where decoy exons resulting from all 4 possible combinations of splice sites were manually added to the reference annotation. Differential splicing analysis using the JCEC model of rMATS indicated lower inclusion of the decoy exon upon SFSWAP knockdown, as expected, but the differences were not statistically significant (Fig. 4c, left). As a control, decoy inclusion levels were significantly higher in either in UPF1 knockdown alone (since the decoy exon form is stabilized) or TG treatment alone (Fig. 4c, middle panels). We reasoned that detection of changes in decoy exon inclusion would be more sensitive in a siSFSWAP/siUPF1 background owing to the presence of the premature stop codon in the decoy exon. Therefore, we performed RNA-seq analysis of SFSWAP knockdown cells (treated with TG) in a UPF1 knockdown background. Alternate splicing analysis using rMATS detected a significant reduction in decoy usage in SFSWAP knockdown cells in this background, consistent with the qPCR results (Fig. 4c, right). Thus, we conclude that SFSWAP promotes inclusion of the OGT decoy exon. Because decoy exon recognition is a critical component of regulation of OGT intron detention, these data further suggest that SFSWAP regulates OGT intron detention by controlling decoy exon inclusion and/or recognition.

SFSWAP may be a global regulator of decoy exon usage

Decoy exons have been proposed to regulate intron retention in a large number of genes in addition to OGT, especially those with longer retained introns (16). To examine whether SFSWAP regulates decoy exon mediated intron retention in genes other than OGT, we re-analyzed our UPF1 knockdown RNA-seq dataset to account for these decoys. Most decoy exons remain uncharacterized to date with the exception of a few like those in OGT (9, 16), ARGLU1 (18) and SF3B1 (16). To obtain annotations

corresponding to putative decoy exons, we used coordinates of novel unannotated cassette exons identified in human erythroblasts by Parra et al (2018). We also obtained a matching list of known retained introns in the same cells identified based on RNA-seq data. We then filtered the list of novel cassette exons to include only those exons whose positions fall entirely within the corresponding retained introns. This list of 2398 novel cassette exons within known retained introns was used as the list of prospective decoy exons (Suppl. Table 3). In principle, all of these may not be splicing decoys, but we think these are reasonable criteria to assay putative decoys.

We examined the role of SFSWAP in regulating the inclusion of these decoys either in a TG-treated or a TG treated UPF1 knockdown background by performing alternate splicing analysis using a human reference annotation supplemented with this list of predicted decoy exons. We observed altered patterns of decoy exon inclusion in SFSWAP knockdown conditions compared to non-target. While the changes in retained intron splicing were primarily in the direction of increased splicing (i.e. less RI inclusion) and that of skipped exon splicing were predominantly in the direction of more inclusion upon SFSWAP knockdown, decoy exons were either more or less included (Fig. 5a). This may reflect the varying mechanisms of action of individual decoys, their splice site strengths, and/or the efficiency of splicing of the intron in which they are found (see Discussion). We further classified these decoy exons based on the predicted translational outcome if the decoys are included in the transcripts (poison cassette, non-poison or untranslated), but we did not see any additional trends for any of these outcome types (Fig. 5b). We obtained similar trends for decoy exon usage regulation by SFSWAP with our TG treated dataset in the absence of UPF1 knockdown (Suppl Fig. S8), with the only major change being the loss of some of the poison exon events (blue dots) with highest fold changes as expected in the absence of a stabilizing UPF1 knockdown. To further investigate the role of SFSWAP in modulating decoy exon usage, we analyzed the effect of SFSWAP knockdown on splicing of decoy exon-containing retained introns. In contrast to the enhanced removal of retained introns for most non-decoy exon-containing events upon SFSWAP knockdown (Fig. 3b and S7), decoy-containing retained intron events did not show a trend towards any direction (Fig. 5c), suggesting a different mechanism of regulation for decoy-containing retained introns.

Consistent with this observation and as observed by other groups (3, 16), we observed a trend towards increased intron length for decoy-containing retained introns compared to non-decoy-containing retained introns (Fig. 5d). Thus, while the mechanism of SFSWAP on individual decoy exons may differ, the data support a role of SFSWAP as a general regulator of decoy exon splicing.

Discussion

Using a genome-wide CRISPR screen, we identified the putative splicing factor SFSWAP to be necessary for efficient OGT IR. The effect is particularly evident in conditions of high O-GlcNAc that strongly favor retention of intron 4. Additionally, we show that depletion of SFSWAP using siRNAs decreases IR in many transcripts and that skipped exons tend to be more included in these conditions. These observations are wholly consistent with previously published single gene focused studies examining splicing of Tau, fibronectin, CD45 and SFSWAP splicing (21, 22, 30). Together, these results strongly support the conclusion that SFSWAP is a splicing factor that primarily functions as a negative regulator of splicing.

In addition, our work suggests that SFSWAP may control OGT splicing by regulating function of its decoy exon and that this may extend to other transcripts with decoy exons. OGT intron 4 and other retained introns require decoy exons for their regulation. Exactly how decoy exons function remains unclear, but several observations suggest that they promote assembly of splicing factors, but not splicing, in order to promote intron retention (9, 16-18). First, mutation of the weak 5´ splice sites of the OGT decoy exon leads to constitutive splicing of exons 4 and 5 in reporters. Second, addition of a morpholino antisense oligonucleotide targeting the OGT decoy's 5´ splice site also promotes constitutive splicing of exon 4-5. Third, placing decoy exons and their flanking sequences into other heterologous introns leads to intron retention, indicating that there is not a gene or intron-specific suppression of splicing. Fourth, CRISPR deletion of the endogenous locus containing the OGT decoy leads to constitutive splicing of exons 4 and 5. Fifth, only a small percentage of mature transcript spliced isoforms splice in the decoy, even when assayed in NMD-inhibiting condition (Fig. 4b). Together, these data

support the recent proposed models that decoy exons require recognition by the spliceosome but are rarely spliced into the final product.

While the mechanism of SFSWAP regulation remains unclear, these characteristics of decoy exons suggest that it functions downstream of exon definition. If SFSWAP suppresses assembly of splicing factors on exons, knockdown of SFSWAP would increase decoy exon definition and thereby increase intron retention of OGT. In addition, increased recognition of the decoy exon may also increase decoy exon inclusion due to better recruitment of splicing factors assembly on the decoy. Our data show the exact opposite of these predictions as splicing of exons 4-5 increase upon SFSWAP depletion and decoy inclusion decreases (Fig. 2, Fig. 4, Fig. 5).

For these reasons, we favor a model in which SFSWAP functions subsequent to exon definition to repress a downstream event in the splicing cycle (Fig. 6). For skipped exons and retained introns without decoys, SFSWAP represses splicing at canonical sites which can then be used upon SFSWAP depletion. Perhaps its RS domain acts as a negative regulator by competing with RS domains from canonical SR proteins that promote splicing. For OGT, we speculate that SFSWAP represses inclusion of the decoy and, in doing so, indirectly inhibits splicing of exons 4 and 5, but promoting stable unproductive assembly of the spliceosome. One piece of data that seems to contradict this model is that there is less splicing of the decoy upon SFSWAP depletion (Fig. 4). We speculate that loss of decoy splicing inhibition by SFSWAP allows competition between the OGT decoy and the exon 4-5 splice sites. Because the latter are stronger sites, decoy inclusion may be lost due to the increase in mRNA production (Fig. 2). Interestingly, for skipped exons and retained introns more generally, SFSWAP knockdown had a clear tendency to increase splicing efficiency (Fig. 3). In contrast, SFSWAP knockdown led to a more equal distribution of inclusion and exclusion events on those retained introns containing potential decoy exons (Fig. 5). Since the putative decoys are generally weaker exons, releasing the negative regulation by SFSWAP may still not be sufficient to promote inclusion of the decoys whereas derepression of canonical skipped exons leads to their inclusion.

Given the absence of canonical RNA binding domains on SFSWAP, it seems plausible that a second protein with direct RNA binding activity mediates its activity. Interestingly, we observed enrichment of known SRSF1 binding motifs at the 5´ end of SFSWAP-dependent differentially regulated retained intron events and around differentially regulated exon skipping events (Suppl. Fig. S9), supporting the idea that SRSF1 acts in concert with SFSWAP to mediate its effect. Alternately, SFSWAP could function in conjunction with the branchpoint binding protein SF1 which has been shown to bind SURP domain containing proteins (like SFSWAP) *in vitro* (20). Notably, we also identified SF1 as a potential target regulating OGT intron retention in our TG-treated CRISPR screen (Fig. 2) and could also validate SFSWAP-SF1 interactions in cell lines by co-immunoprecipitation (Suppl. Fig. S10), further supporting this idea.

With respect to the role of SFSWAP in mediating changes in OGT intron detention in response to varying O-GlcNAc levels in the cell, we speculate that SFSWAP binding to the U2 snRNP is regulated by cellular O-GlcNAc levels through an unidentified sensor. Multiple phosphorylation events on SFSWAP downstream of this sensor may modulate its binding to U2 snRNP. This is supported by the observation that SFSWAP is one of the most highly differentially phosphorylated proteins in the cell after a short treatment (30 min) with an OGT inhibitor, OSMI-2 (15). Treatment of cells with conditions leading to low O-GlcNAc levels lead to phosphorylation of SFSWAP at multiple residues (primarily S604). We propose that this change in phosphorylation status may regulate its disassociation from U2 snRNP. This then leads to altered recognition of the decoy leading to enhanced removal of the retained intron. On the other hand, high O-GlcNAcylation levels lead to accumulation of an unphosphorylated form of SFSWAP capable of binding to U2 snRNP and mediating decoy exon recognition, leading to intron retention. While we show that SFSWAP plays a major role in regulating OGT intron retention, we also realize that there are likely other factors at play in regulating OGT intron detention, especially given the fact that SFSWAP knockdown does not lead to complete excision of the OGT retained intron as is observed upon deletion of the decoy (9). These factors and their mechanism of action remain a subject for future studies.

Materials and methods

Cell culture and growth conditions

HCT116 and HEK293T cells were maintained in DMEM (Sigma, D5796) with penicillin-streptomycin, 2 mM L-glutamine, and 10% fetal bovine serum (FBS, Sigma, F0926) and grown at 37°C in 5% CO_2. Media was supplemented with Plasmocin (InvivoGen, ant-mpt, 1:10,000) and 50 µg/ml hygromycin (Sigma H3274) as required. 250 µg/ml hygromycin or 1 µg/ml of puromycin (Sigma P8833) was used for selection of cells. 293A-TOA cells (34) were grown similarly, but with Tet-free FBS (Atlanta Biologicals, S10350). Plasmid transfections were performed using TransIT-293 (Mirus bio, MIR 2704) for HEK293 cells or Fugene HD (Promega, E2311) for HCT116 cells according to manufacturer's protocols. For modulation of O-GlcNAc levels, cells were treated with 10 µM OSMI-1 (Sigma SML1621), 1 µM TG (Sigma SML0244), 100 µM DON, 10 mM glucosamine or 50 µM PUGNAc for 6 hours. Glucose deprivation was performed by growing cells in glucose-free media (ThermoFisher Scientific, 11966025) for 24 hours. A list of key resources and primer sequences is provided in Suppl. Tables 4 and 5 respectively.

O-GlcNAc responsive GFP reporter construction

An 864 bp PCR product encoding the eGFP, the T2A element and a part of β-globin exon 2 was PCR amplified from pNC1330 using the oligomers NC3739 and NC3482 (Acc65I and BamHI ends). A second PCR product (1056 bp) encoding the remaining part of β-globin exon 2, intron 2 and exon 3 was PCR amplified from pNC980 using NC2085 and NC3851 (BamHI and XbaI ends). The two fragments were ligated into an Acc65I XbaI digested pcDNA3 vector to obtain a BamHI site at the junction of the two fragments. A 4008 bp BamHI fragment encoding OGT exon 4, intron 4 and exon 5 from pNC980 was then ligated into the newly generated BamHI site to obtain a pcDNA version of the GFP reporter. The entire reporter region consisting of eGFP, T2A, OGT exon 4, intron 4, exon 5 and flanking β-globin introns and exons was then moved to pNC1049 using the Acc65I XbaI sites to obtain the final reporter construct (pNC1771).

AAVS1 integration and clonal cell line generation

The reporter construct generated above was integrated into the AAVS1 safe harbor locus of HCT116 cells by TALEN mediated recombination as described before (35). hAAVS1 1L TALEN and hAAVS1 1R TALEN were gifts from Feng Zhang (Addgene plasmid #35431 and #35432 respectively)(26). Reporter integrated cells were selected by growth in 250 µg/ml hygromycin for two weeks. Fluorescence activated cell sorting was performed to select cells expressing varying GFP levels, which were expanded and screened for reporter activity in the presence of either OSMI-1 or TG by northern blot analysis. Cell lines showing enhanced intron 4 splicing in response to OSMI-1 and increased retention of the reporter RNA in response to TG were selected for further screening by RT-qPCR.

Reporter validation

For RT-qPCR validation, total RNA isolated from inhibitor treated cells was subjected to reverse transcription using 2.5 µM dT_{20} oligomers and 200U of SuperScript II reverse transcriptase (ThermoFisher Scientific, 18064014). The resulting cDNA was used as a template for PCR amplification using NC3378 (binding within the GFP ORF) and NC2094 (binding downstream of the last of β-globin exon 3). An amplicon size of 1251 bp is expected in the absence of any unexpected alternate splicing events. For validation of O-GlcNAc responsiveness, the reporter line was treated with modulators of O-GlcNAc levels as above. Cells were subjected to either FACS analysis or western blot analysis using either anti-GFP antibodies or O-GlcNAc RL2 antibodies. β-actin antibodies were used for loading controls.

Northern blot analysis

Northern blot analysis was performed using standard techniques. Briefly, about 3-5 µg of total RNA was resolved on a 0.8-1.4% formaldehyde agarose gel, transferred to a positively changed nylon membrane by capillary transfer, UV-crosslinked and probed with radiolabeled RNA probes generated by *in vitro* transcription with T7 RNA polymerase. Sequences of DNA oligomers used to generate transcript specific probes are listed in Supplementary table 5.

siRNA knockdown

For SFSWAP knockdowns, 293A-TOA were transfected with 40 nM siRNA using RNAiMAX (ThermoFisher Scientific, 13778150) following the manufacturer's protocol. Cells were split 24 hours post-transfection and allowed to grow for an additional 4 days. All other gene knockdowns were performed similarly with 30 nM siRNA and 3 additional days of growth after splitting.

CRISPR screens

Unbiased pooled CRISPR screens using the Human Brunello CRISPR knockout pooled library (a gift from David Root and John Doench, Addgene #73179)(27) were performed as before (35). Briefly, amplified library DNA isolated from ElectroMAX Stbl4 Competent Cells (ThermoFisher Scientific, 11635018) was used to generate a high-titer lentiviral library using HEK293T cells. Following viral titer estimation by CellTiter-Glo Luminescent Cell Viability Assay (Promega, G7570) and Benzonase (Sigma, E1014) treatment, the lentiviral supernatant was used to infect reporter cells at a 30% infection ratio. Pilot screens were performed at 100X library coverage and replicate screens were performed at 300X coverage. Infected cells were selected in puromycin for a total of 8 days. On the last day of selection, cells were either left untreated or treated with either TG (replenished every 12 hours for a total of 24 hours) or OSMI-1 for 24 hours. In the case of TG-treated screens, the high GFP-expressing population of cells were collected, while in case of the OSMI-1-treated screens, low GFP-expressing cells were collected. In the case of untreated screens, both populations of cells were collected. Sorting was performed at the Flow Cytometry Core at UT Southwestern Medical Center. Following DNA isolation and PCR amplification of the guide RNA-encoding locus, next-generation sequencing was performed on an Illumina NextSeq550 instrument using an indexed single-end sequencing protocol with a read length of 75 bp. The original DNA preparation used to generate the lentiviral library was sequenced simultaneously to ensure complete library representation. Reads were mapped to the Brunello library guide RNA sequences and statistical analysis to calculate enrichment over unselected cells was performed using the MAGeCK-VISPR (36) pipeline.

Validation of CRISPR screen hits

Genes corresponding to the top enriched guide RNAs from the TG-treated CRIPSR screen were validated as regulators of OGT intron detention by siRNA-mediated knockdown of the gene in the presence of TG followed by RT-qPCR of relevant junctions of endogenous OGT. Target genes were further validated by northern blot analysis of either the reporter RNA or endogenous OGT RNA following knockdown.

RT-qPCR analysis

For RT-qPCR analysis of endogenous OGT splicing, 1 µg of total RNA was used for reverse transcription using 2.5 µM dT_{20} and 200U of M-MuLV Reverse Transcriptase (NEB, M0253S) for 50 min at 42 °C. Following heat denaturation at 80 °C for 10 min, excess RNA and RNA:DNA hybrids were removed by digestion with RNase A and RNase H. The resulting cDNA was used as a template for qPCR using the iTaq Universal SYBR Green Supermix (Biorad, 1725121). PCR was performed for 40 cycles with an annealing temperature of 60 °C. Analysis was performed using the ΔΔCt method using actin for normalization. OGT decoy exon qPCRs were performed similarly in a UPF1 knockdown background, but with 5 µg of total RNA, 200U of SuperScript IV (ThermoFisher Scientific, 18090050) and a mixture of 2.5 µM dT_{20} and 2 pmol of an OGT exon 5 specific reverse primer (NC985).

RNA-seq analysis

RNA-seq analysis was performed in 293A-TOA cells in either wild-type or UPF1 knockdown background with or without 1 µM TG treatment for 6 hours. Cells were harvested from 6-well plates in three biological replicates at 70-80% confluency. Knockdown efficiency of proteins of interest were validated by either western blot analysis or RT-qPCR with appropriate primers (Suppl. Fig. S11-S14). RNA isolation was performed using Zymo Direct-zol RNA miniprep kit (Zymo R2050). One µg of total RNA was used for polyA-RNA isolation and library preparation using the KAPA mRNA Hyperprep kit (Roche, KK8580) following the manufacturer's protocol. RNA was fragmented to an average fragment size of 100 bp. The kit-supplied adaptor was replaced with NEB adaptors and index primers (NEB, E7335S) to enable pooling of

multiple samples per flow cell. Single-end sequencing with a read length of 100 bp was performed using an Illumina NextSeq 2000 instrument at the McDermott Center Next Generation Sequencing (NGS) Core at UT Southwestern Medical Center to obtain 60-65 million reads per sample on average.

Reads were trimmed with cutadapt and aligned to GENCODE release 40 of the human reference genome with STAR (version 2.7)(37) using the '--twopassMode Basic' option. Batch correction was performed, if necessary, using the EDASeq (38) and RUVSeq (39) R packages. Differential expression analysis was performed using edgeR (40) using factors of unwanted variation obtained from RUVSeq as an additional covariate in the design matrix.

Alternate splicing analysis

Alternate splicing analysis was performed using rMATS (29), MAJIQ (32) and Whippet (33). For rMATS, events with FDR <= 0.05 and IncLevelDifference >= 0.2 were considered significant. For Whippet and MAJIQ, events with probability >= 0.9 and ΔPSI of 20% and 10% respectively were considered significant. The proportion of event types as a fraction of all event types was plotted from rMATS output (JC model) using MASER (https://github.com/DiogoVeiga/maser). GC content calculations were performed based on rMATS JC model outputs taking only significant events (as defined above) into consideration. Enrichment of RBP binding sites around alternately spliced events was visualized using the rMAPS2 web server (41) with rMATS JCEC model output files provided as inputs. Sashimi plots for regions of interest were generated using rmats2sashimiplot (https://github.com/Xinglab/rmats2sashimiplot).

Amplicon sequencing

cDNA preparations from TG-treated SFSWAP knockdown (or non-target) cells in a UPF1 knockdown background were used as templates for PCR amplification of the region between OGT exon 3 and exon 8 using the primers NC1769 and NC988. PCR was performed for 30 cycles using Q5 DNA polymerase (NEB, M0491S). The amplicons were sequenced at Plasmidsaurus. Sequencing reads were aligned to a version of OGT cDNA sequence containing the longest form of the OGT decoy exon (153 bp) but

excluding the rest of the retained intron using minimap2 (42) and the number of reads overlapping the decoy exon were computed using bedtools (43).

Global alternate decoy exon usage analysis

Decoy exon usage analysis was performed using RNA-seq reads obtained with or without UPF1 knockdown in the presence of TG, and either non-target (siNT) or SFSWAP (siSFSWAP) knockdown. To obtain decoy exon annotations, we used coordinates of novel unannotated cassette exons identified in human erythroblasts by Parra et al. based on a set of stringent criteria (16). This list of novel cassette exons was further filtered to only keep cassettes located within known retained introns in the same cell line. The coordinates of these novel cassette exons located within known retained introns were used to supplement RefSeq (based on genome assembly GCF_000001405.34/GRCh38.p8) to obtain a version of the human reference annotation containing potential decoy exons. RNA-seq reads were trimmed and mapped to this modified reference using STAR in 'two-pass Basic' mode. rMATS analysis was performed as above.

Co-immunoprecipitation analysis

Co-immunoprecipitation of SFSWAP with SF1 was performed from 293A-TOA cells grown in a 60 mm plate treated with either DMSO, TG or OSMI-1. Briefly, cells were lysed in a buffer containing 100 mM NaCl, 2.5 mM $MgCl_2$, 10 mM Tris-HCl pH 7.5 and 0.5 % IGEPAL CA-630, 1 mM PMSF and 1X Protease Inhibitor Cocktail Set V (Millipore, 539137). Samples were nutated at room temperature with 20U RQ1 DNase (Promega, M6101) and RNase A (10 µg/ml) for 15 min, clarified by centrifugation, and incubated with 2 µg of mouse anti-SF1 antibodies for 2 hours at 4 °C. The antibody complexes were pulled down with 20 µl protein A magnetic beads, washed 5 times with the same buffer lacking protease inhibitors and eluted with 1X SDS-PAGE loading buffer. The eluate was resolved on a 7.5% SDS-PAGE gel, transferred to a nylon membrane, probed with rabbit anti-SFSWAP antibodies (1:1000) and detected using IRDye-conjugated secondary antibodies on a Licor instrument.

Identification of SFSWAP interacting proteins

Immunoprecipitation-Mass spectrometry (IP-MS) analysis to identify SFSWAP interacting proteins was performed using HEK239 cells transiently overexpressing an N-terminally Myc-tagged version of SFSWAP. Cells were lysed and clarified as above and SFSWAP was pulled down with 20 µl of Myc-trap magnetic agarose beads (Chromotek, ytma). The beads were washed as above with 2 additional washes excluding IGEPAL CA-630. Proteins were eluted using 2X Myc peptide (Chromotek, 2yp) following manufacturer's protocols. The samples were resolved 1 cm into a 4-20% precast TGX gel (Biorad, 4561093), stained, excised and submitted to UT Southwestern Proteomics Core for further analysis. Trypsin digestion, mass spectrometric analysis (in an Orbitrap Fusion Lumos instrument with a 90 min HPLC gradient), database search and comparative analysis using Proteome Discoverer 3.0 were performed by the facility.

Acknowledgments

We thank Drs. Didier Trono, Feng Zhang, David Root, and John Doench for plasmids. We also thank the UT Southwestern Flow Cytometry Core, Proteomics Core and the McDermott Center Next Generation Sequencing Core for assistance with experiments. This research was supported by the National Institutes of Health R01 GM127311, U01 CA242115, R01 AI153175, and R01 AI123165.

Data availability

Raw sequencing reads for all sequencing experiments described in this paper have been deposited in NCBI GEO with the accession number GSE277952.

References

1. G. Monteuuis, J. J. L. Wong, C. G. Bailey, U. Schmitz, J. E. J. Rasko, The changing paradigm of intron retention: regulation, ramifications and recipes. *Nucleic Acids Res* **47**, 11497-11513 (2019).
2. D. Rekosh, M. L. Hammarskjold, Intron retention in viruses and cellular genes: Detention, border controls and passports. *Wiley Interdiscip Rev RNA* **9**, e1470 (2018).
3. P. L. Boutz, A. Bhutkar, P. A. Sharp, Detained introns are a novel, widespread class of post-transcriptionally spliced introns. *Genes Dev* **29**, 63-80 (2015).
4. U. Braunschweig *et al.*, Widespread intron retention in mammals functionally tunes transcriptomes. *Genome Res* **24**, 1774-1786 (2014).
5. K. Yap, Z. Q. Lim, P. Khandelia, B. Friedman, E. V. Makeyev, Coordinated regulation of neuronal mRNA steady-state levels through developmentally controlled intron retention. *Genes Dev* **26**, 1209-1223 (2012).
6. K. E. Pendleton, S. K. Park, O. V. Hunter, S. M. Bresson, N. K. Conrad, Balance between MAT2A intron detention and splicing is determined cotranscriptionally. *RNA* **24**, 778-786 (2018).
7. O. Mauger, F. Lemoine, P. Scheiffele, Targeted Intron Retention and Excision for Rapid Gene Regulation in Response to Neuronal Activity. *Neuron* **92**, 1266-1278 (2016).
8. K. Ninomiya, N. Kataoka, M. Hagiwara, Stress-responsive maturation of Clk1/4 pre-mRNAs promotes phosphorylation of SR splicing factor. *J Cell Biol* **195**, 27-40 (2011).
9. S. K. Park *et al.*, A Conserved Splicing Silencer Dynamically Regulates O-GlcNAc Transferase Intron Retention and O-GlcNAc Homeostasis. *Cell Rep* **20**, 1088-1099 (2017).
10. L. K. Kreppel, M. A. Blomberg, G. W. Hart, Dynamic glycosylation of nuclear and cytosolic proteins. Cloning and characterization of a unique O-GlcNAc transferase with multiple tetratricopeptide repeats. *J Biol Chem* **272**, 9308-9315 (1997).

11. W. A. Lubas, D. W. Frank, M. Krause, J. A. Hanover, O-Linked GlcNAc transferase is a conserved nucleocytoplasmic protein containing tetratricopeptide repeats. *J Biol Chem* **272**, 9316-9324 (1997).
12. M. R. Bond, J. A. Hanover, A little sugar goes a long way: the cell biology of O-GlcNAc. *J Cell Biol* **208**, 869-880 (2015).
13. M. P. Mannino, G. W. Hart, The Beginner's Guide to O-GlcNAc: From Nutrient Sensitive Pathway Regulation to Its Impact on the Immune System. *Front Immunol* **13**, 828648 (2022).
14. Y. Gao, L. Wells, F. I. Comer, G. J. Parker, G. W. Hart, Dynamic O-glycosylation of nuclear and cytosolic proteins: cloning and characterization of a neutral, cytosolic beta-N-acetylglucosaminidase from human brain. *J Biol Chem* **276**, 9838-9845 (2001).
15. Z. W. Tan *et al.*, O-GlcNAc regulates gene expression by controlling detained intron splicing. *Nucleic Acids Res* **48**, 5656-5669 (2020).
16. M. Parra *et al.*, An important class of intron retention events in human erythroblasts is regulated by cryptic exons proposed to function as splicing decoys. *RNA* **24**, 1255-1265 (2018).
17. M. Parra, W. Zhang, J. Vu, M. DeWitt, J. G. Conboy, Antisense targeting of decoy exons can reduce intron retention and increase protein expression in human erythroblasts. *RNA* **26**, 996-1005 (2020).
18. S. P. Pirnie, A. Osman, Y. Zhu, G. G. Carmichael, An Ultraconserved Element (UCE) controls homeostatic splicing of ARGLU1 mRNA. *Nucleic Acids Res* **45**, 3473-3486 (2017).
19. F. Denhez, R. Lafyatis, Conservation of regulated alternative splicing and identification of functional domains in vertebrate homologs to the Drosophila splicing regulator, suppressor-of-white-apricot. *J Biol Chem* **269**, 16170-16179 (1994).
20. A. Crisci *et al.*, Mammalian splicing factor SF1 interacts with SURP domains of U2 snRNP-associated proteins. *Nucleic Acids Res* **43**, 10456-10473 (2015).

21. J. Wang *et al.*, Tau exon 10, whose missplicing causes frontotemporal dementia, is regulated by an intricate interplay of cis elements and trans factors. *J Neurochem* **88**, 1078-1090 (2004).
22. M. Sarkissian, A. Winne, R. Lafyatis, The mammalian homolog of suppressor-of-white-apricot regulates alternative mRNA splicing of CD45 exon 4 and fibronectin IIICS. *J Biol Chem* **271**, 31106-31114 (1996).
23. A. M. Scarborough, A. Govindan, N. K. Conrad, "Genome-Wide CRISPR Screening to Identify Mammalian Factors that Regulate Intron Retention" in Alternative Splicing: Methods and Protocols, P. Scheiffele, O. Mauger, Eds. (Springer US, New York, NY, 2022), 10.1007/978-1-0716-2521-7_16, pp. 263-284.
24. M. L. L. Donnelly *et al.*, The 'cleavage' activities of foot-and-mouth disease virus 2A site-directed mutants and naturally occurring '2A-like' sequences. *J Gen Virol* **82**, 1027-1041 (2001).
25. M. L. L. Donnelly *et al.*, Analysis of the aphthovirus 2A/2B polyprotein 'cleavage' mechanism indicates not a proteolytic reaction, but a novel translational effect: a putative ribosomal 'skip'. *J Gen Virol* **82**, 1013-1025 (2001).
26. N. E. Sanjana *et al.*, A transcription activator-like effector toolbox for genome engineering. *Nat Protoc* **7**, 171-192 (2012).
27. J. G. Doench *et al.*, Optimized sgRNA design to maximize activity and minimize off-target effects of CRISPR-Cas9. *Nat Biotechnol* **34**, 184-191 (2016).
28. W. Li *et al.*, MAGeCK enables robust identification of essential genes from genome-scale CRISPR/Cas9 knockout screens. *Genome Biol* **15**, 554 (2014).
29. S. Shen *et al.*, rMATS: robust and flexible detection of differential alternative splicing from replicate RNA-Seq data. *Proc Natl Acad Sci U S A* **111**, E5593-5601 (2014).
30. Z. Zachar, T. B. Chou, P. M. Bingham, Evidence that a regulatory gene autoregulates splicing of its transcript. *EMBO J* **6**, 4105-4111 (1987).
31. Z. Zachar, T. B. Chou, J. Kramer, I. P. Mims, P. M. Bingham, Analysis of autoregulation at the level of pre-mRNA splicing of the suppressor-of-white-apricot gene in Drosophila. *Genetics* **137**, 139-150 (1994).

32. J. Vaquero-Garcia *et al.*, RNA splicing analysis using heterogeneous and large RNA-seq datasets. *Nat Commun* **14**, 1230 (2023).
33. T. Sterne-Weiler, R. J. Weatheritt, A. J. Best, K. C. H. Ha, B. J. Blencowe, Efficient and Accurate Quantitative Profiling of Alternative Splicing Patterns of Any Complexity on a Laptop. *Mol Cell* **72**, 187-200 e186 (2018).
34. B. B. Sahin, D. Patel, N. K. Conrad, Kaposi's sarcoma-associated herpesvirus ORF57 protein binds and protects a nuclear noncoding RNA from cellular RNA decay pathways. *PLoS Pathog* **6**, e1000799 (2010).
35. A. M. Scarborough *et al.*, SAM homeostasis is regulated by CFI(m)-mediated splicing of MAT2A. *Elife* **10** (2021).
36. W. Li *et al.*, Quality control, modeling, and visualization of CRISPR screens with MAGeCK-VISPR. *Genome Biol* **16**, 281 (2015).
37. A. Dobin *et al.*, STAR: ultrafast universal RNA-seq aligner. *Bioinformatics* **29**, 15-21 (2013).
38. D. Risso, K. Schwartz, G. Sherlock, S. Dudoit, GC-content normalization for RNA-Seq data. *BMC Bioinformatics* **12**, 480 (2011).
39. D. Risso, J. Ngai, T. P. Speed, S. Dudoit, Normalization of RNA-seq data using factor analysis of control genes or samples. *Nat Biotechnol* **32**, 896-902 (2014).
40. M. D. Robinson, D. J. McCarthy, G. K. Smyth, edgeR: a Bioconductor package for differential expression analysis of digital gene expression data. *Bioinformatics* **26**, 139-140 (2010).
41. J. Y. Hwang *et al.*, rMAPS2: an update of the RNA map analysis and plotting server for alternative splicing regulation. *Nucleic Acids Res* **48**, W300-W306 (2020).
42. H. Li, Minimap2: pairwise alignment for nucleotide sequences. *Bioinformatics* **34**, 3094-3100 (2018).
43. A. R. Quinlan, I. M. Hall, BEDTools: a flexible suite of utilities for comparing genomic features. *Bioinformatics* **26**, 841-842 (2010).
44. N. E. Sanjana, O. Shalem, F. Zhang, Improved vectors and genome-wide libraries for CRISPR screening. *Nat Methods* **11**, 783-784 (2014).

45. M. I. Love, W. Huber, S. Anders, Moderated estimation of fold change and dispersion for RNA-seq data with DESeq2. *Genome Biol* **15**, 550 (2014).

Figure Legends

Fig. 1. Construction of an O-GlcNAc responsive GFP biosensor.

a. Schematic of the GFP reporter (left, drawn to scale) and predicted changes in reporter splicing and expression upon varying cellular O-GlcNAc conditions (right). ISS – Intronic splicing silencer; LHA – Left homology arm; RHA – Right homology arm; HBB – Hemoglobin subunit β; PGK – Phosphoglycerokinase; CMV – Cytomegalovirus; bGH – Bovine growth hormone; SV40 – Simian virus 40.
b. Semi-quantitative RT-PCR of RNA isolated from the reporter line under different treatment conditions using DNA primers (NC3378 and NC2094) that hybridize within the GFP ORF and just upstream of the polyadenylation signal sequence as shown below. The PCR conditions make it unlikely to detect the full-length detained intron isoform, so only the mRNA is observed.
c. Northern blot analysis of total RNA isolated from the reporter line after treatment with either DMSO, 1 μM TG or 10 μM OSMI-1 for 6 hours. The blot was probed for GFP. The retained intron band is heterogeneous and difficult to discern clearly due to its co-migration with the large ribosomal RNA. Methylene blue stain of the blot (right) is shown as a loading control.
d. GFP fluorescence levels of the reporter line as measured by flow cytometry after treatment with DMSO, TG or OSMI-1 for 24 hours.
e. Validation of GFP reporter protein levels by western blot analysis after treatment of the reporter line with various modulators of cellular O-GlcNAc levels (left). Steps in the hexosamine biosynthesis pathway targeted by the modulators are shown on the right. Treatment with modulators indicated in red are expected to lead to reduced cellular O-GlcNAc levels, while treatment with those indicated in green are expected to lead to increased cellular O-GlcNAc levels. A broad specificity O-GlcNAc antibody (RL2) and β-actin are used as controls.
f. Northern blot analysis of RNA isolated from either 30 nM non-target (siNT) or OGT specific (siOGT) siRNA-treated reporter line. Cells were treated for 6 hr with DMSO, TG or OSMI-1 3 days after siRNA treatment. The blot was probed for GFP as above.

Fig. 2. SFSWAP is a negative regulator of OGT intron 4 splicing.

a. Top, timeline of CRISPR screen. Bottom, MAGeCK analysis of CRIPSR screen results from TG-treated gain of GFP screen in three biological replicates. Top hits are color coded based on predicted function of the protein. Target genes are arranged alphabetically on the x-axis.
b. GFP fluorescence of TG-treated reporter cells 4 days post treatment with siRNA corresponding to non-target (siNT), OGT (siOGT) or SFSWAP (siSFSWAP).
c. Northern blot analysis of RNA isolated from either the TG-treated reporter line (left, probed for GFP) or TG-treated 293A-TOA cells (right, probed for OGT) 4 days after treatment with siRNA corresponding to either non-target (siNT) or SFSWAP (siSFSWAP). Cells were treated with TG for 6 hours just before RNA isolation.
d. RT-qPCR analysis of the splice junctions of interest after treatment of cells with either DMSO, TG or OSMI-1 in the presence or absence of SFSWAP knockdown (n=3). Primers used correspond to either the OGT intron 4 spliced junction (e4-e5) or retained intron junction (RI-e5).

Fig. 3. SFSWAP is a global regulator of retained intron splicing and exon skipping.

a. Alternate splicing analysis in untreated SFSWAP knockdown (siSFSWAP) cells compared to non-target (siNT)-treated cells using rMATS (n=3). The number of events of each type are plotted as proportion of total events detected. A3SS – alternate 3´ splice site; A5SS – alternate 5´ splice site; MXE – mutually exclusive exon; RI – retained intron; SE – skipped exon. Assignment of sample labels for events was done based on the value of IncLevelDifference (events with positive IncLevelDifference were designated as siNT and negative IncLevelDifference were designated as siSFSWAP).

b. Scatter plots of retained intron (RI) and skipped exon (SE) events plotted using the JC model of rMATS (top). The difference in inclusion values between siNT and siSFSWAP-treated cells is plotted on the x-axis. Only statistically significant events (FDR <= 0.05) are shown. Violin plots of inclusion levels corresponding to the individual samples are shown below. Median inclusion value for the sample is indicated by the black dot. Only significant events with 20% or greater change in inclusion levels are plotted for the violin plots.
c. IGV screenshot of read coverages of a few significant retained intron events. The intron of interest is marked by the red rectangle.
d. GC content of relevant regions of significant RI and SE events (FDR <= 0.05, >= 10% change in inclusion levels). Red bars indicate the mode of GC content in each region.

Fig. 4. SFSWAP regulates OGT decoy exon inclusion.

a. RT-qPCR analysis of OGT intron 4 splicing in UPF1 knockdown background. SFSWAP knockdown was performed for 5 days and cells were then treated with TG for 6 hours before RNA isolation and reverse transcription using a mixture of dT_{20} and a DNA oligomer complementary to exon 5 of OGT. qPCR was performed for either the spliced junction (e4-e5), retained intron junction (RI-e5) or decoy-e5 junction as shown. DE – decoy exon.
b. IGV screenshot of aligned reads after nanopore sequencing of semi-quantitative RT-PCR amplicons generated from the above samples using DNA oligomers complementary to exon 3 and exon 8 of OGT. A zoomed version is shown below to better show changes in the decoy exon region.
c. Quantification of OGT decoy exon inclusion from RNA-seq data in the presence or absence of UPF1 knockdown and/or TG treatment. Inclusion levels and p-values are calculated from the JCEC model of rMATS performed after alignment against a custom reference annotation of the human genome containing decoy exon annotations.

Fig. 5. SFSWAP is a global regulator of decoy exon splicing.

a. Scatter plot of global decoy exon inclusion level changes upon SFSWAP knockdown in a TG-treated UPF1 knockdown background. Significant events with greater than 20% change in inclusion levels are colored. Not all analyzed cassettes may function as splicing decoys.
b. Exon types of the events shown in (a) classified based on the predicted translation outcome. Events shown in blue introduce an in-frame stop codon in the CDS, thus functioning as poison cassettes.
c. Inclusion level changes in decoy-containing retained introns upon SFSWAP knockdown in a TG-treated UPF1 knockdown background. Significant events with 10% or greater change in inclusion levels are colored.
d. Length distribution of the decoy-containing retained introns compared to non-decoy containing retained introns.

Fig. 6. Model for the mechanism of action of SFSWAP on intron retention and exon skipping. See text for details. In the case of retained introns without decoy exons or cassette exons (top and middle), SFSWAP (green oval) restricts splicing subsequent to definition of the exons by U1 and U2. For retained introns with decoys, this inhibition of decoy exon inclusion is linked to the decoy exon's function to promote intron retention. For simplicity, we showed SFSWAP functioning in combination with U2 snRNP, but it could also be functioning at the 5´ splice sites (see Discussion).

Fig. S1. CRISPR screen for the identification of factors regulating OGT intron detention in the absence of TG treatment (n=1). Results of MAGeCK analysis are plotted with target genes arranged alphabetically on the x-axis.

Fig. S2. Validation of targets identified in the TG-treated CRISPR screen by RT-qPCR analysis of endogenous OGT intron 4 splicing after knockdown of the target of interest

(n=2). Percent spliced OGT RNA was calculated as the ratio of spliced OGT mRNA (exon 4-exon 5 junction) to the sum of spliced and retained (RI-exon 5 junction) forms of the transcript. RNA knockdowns were not verified by western blot or RT-qPCR, so negative results are interpreted to be inconclusive.

Fig. S3. Alternate splicing analysis in SFSWAP knockdown background using Whippet (n=3). Scatter plots of RI and SE events are shown with significant events colored (probability >=0.9 and greater than or equal to 20% change in ΔPSI). Violin plots of PSI distribution of significant events from individual samples is shown below. The black dot corresponds to the median PSI value of each sample.

Fig. S4. Alternate splicing analysis in SFSWAP knockdown background using MAJIQ (n=3). Scatter plots of RI and SE events are shown with significant events colored (probability >=0.9 and greater than or equal to 10% change in ΔPSI). Violin plots of PSI distribution of significant events from individual samples is shown below. The black dot corresponds to the median PSI value of each sample.

Fig. S5. IGV screenshot of read coverage of the OGT transcript from RNA-seq analysis in the presence or absence of SFSWAP knockdown (n=3) without any inhibitor treatment.

Fig. S6. Sashimi plot of splice events around the OGT retained intron showing enhanced removal of the retained intron upon SFSWAP knockdown. Splicing to generate the mature mRNA (e4-e5) is shown in green.

Fig. S7. Scatter plot of significant RI and SE events from rMATS analysis of RNA-seq data from TG-treated cells in the presence or absence of SFSWAP knockdown.

Fig. S8.

a. Scatter plot of global decoy exon inclusion level changes upon SFSWAP knockdown in a TG-treated background. Significant events with greater than 20% change in inclusion levels are colored.
b. Exon types of the events shown in (a) classified based on the predicted translation outcome. Events shown in blue introduce an in-frame stop codon in the CDS, thus functioning as poison cassettes.
c. Inclusion level changes in decoy-containing retained introns upon SFSWAP knockdown in TG-treated cells. Significant events with 10% or greater change in inclusion levels are colored.
d. Length distribution of the decoy-containing retained introns compared to non-decoy containing retained introns.

Fig. S9. Enrichment of different SRSF1 binding sites on significant alternate splicing events as analyzed by rMAPS. Enrichment on RI and SE events is shown as a motif score across the regions of interest. Colored solid lines (red or blue) correspond to motif scores for upregulated and downregulated events respectively, and dotted lines indicate corresponding -log(p-values). The solid black line indicates the background motif score for the region.

Fig. S10. Co-immunoprecipitation (co-IP) analysis of SF1 interaction with SFSWAP. SF1 was immunoprecipitated with mouse anti-SF1 antibodies from 293A-TOA cells treated with either DMSO, TG or OSMI-1 and the blot was probed with rabbit anti-SFSWAP antibodies. The ~150 kDa band corresponding to SFSWAP is marked. Notably, IP efficiency does not change upon treatment with TG or OSMI-1.

Fig. S11. Validation of SFSWAP knockdown for untreated RNA-seq samples (data shown in Fig. 3) by western blot analysis (top) and corresponding quantification (normalized to actin, bottom). siRNA #1 is not an effective siRNA.

Fig. S12. IGV screenshot showing knockdown of SFSWAP in the untreated RNA-seq samples (data shown in Fig. 3).

Fig. S13. Validation of SFSWAP and UPF1 knockdown in TG-treated RNA-seq samples in the presence or absence of UPF1 knockdown (data shown in Figs. 4 and 5) by RT-qPCR.

Fig. S14. IGV screenshot showing knockdown of SFSWAP in the TG-treated RNA-seq samples in the presence (bottom) or absence (top) of UPF1 knockdown (data shown in Figs. 4 and 5).

Table S1. Full list of putative target genes identified by MAGeCK analysis of TG-treated gain of GFP CRISPR screen (n=3).

Table S2. Full list of putative target genes identified by MAGeCK analysis of untreated gain of GFP CRISPR screen (n=1).

Table S3. List of potential decoy exons analyzed in Fig. 5.

Table S4. Table of key resources used in the paper.

Table S5. List of primers used.

Supplementary Table 4. Key resources

Reagent type (species) or resource	Designation	Source or reference	Identifiers	Additional information
Cell line (*H. sapiens*)	HEK293A-TOA	Dr. Nicholas K. Conrad (34)	UT Southwestern Medical Center	
Cell line (*H. sapiens*)	HEK293T	Dr. Joshua Mendell	UT Southwestern Medical Center	
Cell line (*H. sapiens*)	HCT116	ATCC	CCL-247	
Cell line (*H. sapiens*)	HCT116 GFP-β-OGT	This paper	Clone E9	Maintained by Nicholas K. Conrad lab
Bacterial strain (*E. coli*)	ElectroMAX Stbl4 competent cells	ThermoFisher	Cat #11635018	Competent cells
Bacterial strain (*E. coli*)	DH5α	ThermoFisher	Cat #EC0112	Competent cells
Antibody	Rabbit polyclonal anti-GFP	Abcam	Cat #ab6556; RRID:AB_305564	1:2000
Antibody	Rabbit polyclonal anti-SFSWAP	Bethyl	Cat #A300-985A; RRID:AB_2185354	1:1000
Antibody	Rabbit polyclonal anti-SF1	Abnova	Cat #H00007536-M01; RRID:AB_607016	1:5000
Antibody	Goat anti-rabbit IRDye 800CW	LI-COR Biosciences	Cat #926–32211; RRID:AB_621843	1:10,000
Antibody	Goat anti-mouse IRDye 800CW	LI-COR Biosciences	Cat #926-32210; RRID:AB_621842	1:10,000
Antibody	Mouse monoclonal anti-beta-actin	Abcam	Cat #ab6276; RRID:AB_2223210	1:10,000
Antibody	Mouse monoclonal	Invitrogen	Cat #MA1-072; RRID:AB_326364	1:1000

	anti-O-GlcNAc (RL2)			
Antibody-based Reagent	Myc-Trap magnetic agarose beads	Chromotek	Cat #ytma	
Synthetic Peptide	2x Myc-peptide	Chromotek	Cat #2yp	
Recombinant DNA reagent	Plasmid: pcDNA3	ThermoFisher	Cat #V79020	
Recombinant DNA reagent	Plasmid: psPAX2	Addgene	Plasmid #12260	psPAX2 was a gift from Didier Trono (Addgene plasmid #12260 ; http://n2t.net/addgene:12260 ; RRID:Addgene_12260)
Recombinant DNA reagent	Plasmid: pMD2.G	Addgene	Plasmid #12259	pMD2.G was a gift from Didier Trono (Addgene plasmid #12259 ; http://n2t.net/addgene:12259 ; RRID:Addgene_12259)
Recombinant DNA reagent	Plasmid: lentiCRISPR v2	(44)	Plasmid #52961	lentiCRISPR v2 was a gift from Feng Zhang (Addgene plasmid #52961 ; http://n2t.net/addgene:52961 ; RRID:Addgene_52961)
Recombinant DNA reagent	Brunello pooled library in lentiCRISPR v2	(27)	Pooled Library #73179	Human Brunello CRISPR knockout pooled library was a gift from David Root and John Doench (Addgene #73179)
Recombinant DNA reagent	Plasmid: pc-Myc-SFSWAP	GenScript	Cat #OHu108377	Obtained as an N-terminal Myc-tagged clone
Recombinant DNA reagent	Plasmid: hAAVS1-GFP-T2A-b2-MAT-E8-3 hp2-6m9	(35)	pNC1330	
Recombinant DNA reagent	Plasmid: hAAVS1-GFP-β-OGT	This paper	pNC1771	

Recombinant DNA reagent	hAAVS1 1L TALEN	(26)	Plasmid #35431	hAAVS1 1L TALEN was a gift from Feng Zhang (Addgene plasmid # 35431 ; http://n2t.net/addgene:35431 ; RRID:Addgene_35431)
Recombinant DNA reagent	hAAVS1 1R TALEN	(26)	Plasmid #35432	hAAVS1 1R TALEN was a gift from Feng Zhang (Addgene plasmid # 35432 ; http://n2t.net/addgene:35432 ; RRID:Addgene_35432)
Recombinant DNA reagent	β-OGT	(9)	N/A	β-globin based OGT splicing reporter
Commercial assay or kit	CellTiter-Glo	Promega	Cat #G7570	
Commercial assay or kit	AMPure XP	Beckman Coulter	Cat #A63880	
Commercial assay or kit	KAPA mRNA HyperPrep Kit	Roche	Cat # KK8580	
Sequence-based reagent	Negative Control No. 2 siRNA	ThermoFisher	Cat #4390846	Non-target siRNA
Sequence-based reagent	SFSWAP siRNA #1	ThermoFisher	Assay ID #s12746	Silencer select siRNA
Sequence-based reagent	SFSWAP siRNA #2	ThermoFisher	Assay ID #s12748	Silencer select siRNA
Sequence-based reagent	UPF1 siRNA #1	Sigma-Aldrich	siRNA ID # SASI_Hs01_00101017	Mission siRNA
Sequence-based reagent	UPF1 siRNA #2	Sigma-Aldrich	siRNA ID # SASI_Hs01_00101018	Mission siRNA
Sequence-based reagent	OGT siRNA #1	ThermoFisher	Assay ID #s16094	Silencer select siRNA
Sequence-based reagent	OGT siRNA #2	ThermoFisher	Assay ID #s16095	Silencer select siRNA

Sequence-based reagent	NIPP1 siRNA #1	ThermoFisher	Assay ID #s10954	Silencer select siRNA
Sequence-based reagent	NIPP1 siRNA #2	ThermoFisher	Assay ID #s10955	Silencer select siRNA
Sequence-based reagent	LSM4 siRNA #1	ThermoFisher	Assay ID #s24521	Silencer select siRNA
Sequence-based reagent	LSM4 siRNA #2	ThermoFisher	Assay ID #s24522	Silencer select siRNA
Sequence-based reagent	BCAS2 siRNA #1	ThermoFisher	Assay ID #s20104	Silencer select siRNA
Sequence-based reagent	BCAS2 siRNA #2	ThermoFisher	Assay ID #s20105	Silencer select siRNA
Sequence-based reagent	ELAVL1 siRNA #1	ThermoFisher	Assay ID #s4609	Silencer select siRNA
Sequence-based reagent	ELAVL1 siRNA #2	ThermoFisher	Assay ID #4610	Silencer select siRNA
Sequence-based reagent	HNRNPU siRNA #1	ThermoFisher	Assay ID #s6745	Silencer select siRNA
Sequence-based reagent	HNRNPU siRNA #2	ThermoFisher	Assay ID #s6744	Silencer select siRNA
Sequence-based reagent	ZNF236 siRNA #1	ThermoFisher	Assay ID #s15328	Silencer select siRNA
Sequence-based reagent	ZNF236 siRNA #2	ThermoFisher	Assay ID #s15326	Silencer select siRNA
Sequence-based reagent	ZC3H13 siRNA #1	ThermoFisher	Assay ID #s23011	Silencer select siRNA
Sequence-based reagent	ZC3H13 siRNA #2	ThermoFisher	Assay ID #s23012	Silencer select siRNA
Sequence-based reagent	ZNHIT2 siRNA #1	ThermoFisher	Assay ID #s194322	Silencer select siRNA

Sequence-based reagent	ZNHIT2 siRNA #2	ThermoFisher	Assay ID #s2212	Silencer select siRNA
Sequence-based reagent	SF1 siRNA #1	ThermoFisher	Assay ID #s14976	Silencer select siRNA
Sequence-based reagent	SF1 siRNA #2	ThermoFisher	Assay ID #s200464	Silencer select siRNA
Sequence-based reagent	KIAA1429 siRNA #1	ThermoFisher	Assay ID #s24832	Silencer select siRNA
Sequence-based reagent	KIAA1429 siRNA #2	ThermoFisher	Assay ID #s24833	Silencer select siRNA
Software, algorithm	FlowJo	BD Biosciences	v 10	
Software, algorithm	Snapgene	Dotmatics	v 7.2.1	
Software, algorithm	rMATS	(29)	v 4.3.0	
Software, algorithm	STAR	(37)	v 2.7	
Software, algorithm	Cutadapt	DOI:10.14806/ej.17.1.200	v 1.9.1	
Software, algorithm	FastQC	http://www.bioinformatics.babraham.ac.uk/projects/fastqc/	v 0.11.5	
Software, algorithm	Rstudio	Posit Software	2024.04.1	
Software, algorithm	MAGeCK-VISPR	(36)	v 0.5.6	
Software, algorithm	Whippet	(33)	v 1.6.1	
Software, algorithm	MAJIQ	(32)	v 2.4.dev102	

Software, algorithm	maser	https://github.com/DiogoVeiga/maser	v 1.22.0	
Software, algorithm	bedtools	(43)	v 2.29.0	
Software, algorithm	minimap2	(42)	v 2.26	
Software, algorithm	edgeR	(40)	v 4.2.1	
Software, algorithm	DESeq2	(45)	v 1.44.0	
Software, algorithm	EDASeq	(38)	v 2.38.0	
Software, algorithm	RUVSeq	(39)	v 1.38.0	
Software, algorithm	rMAPS2 web server	(41)	N/A	http://rmaps.cecsresearch.org/
Software, algorithm	rmats2sashimiplot	https://github.com/Xinglab/rmats2sashimiplot	v 3.0.0	
Software, algorithm	Graphpad Prism	Dotmatics	v 10.3.0	

Supplementary Table 5. List of primers

Name	Sequence	Description
NC4540	CCAAGATTACTCCAAGCTACTG	OGT exon 5 reverse primer for RT-qPCR
NC4275	CTGGGTCGCTTGGAAGAAG	OGT exon 4 forward primer for RT-qPCR
NC4273	CCTTTCCCTCCCATCTTCTTTC	OGT RI forward primer for RT-qPCR
NC4278	ACAACCTCCTCCTCCTCTT	OGT decoy forward primer for RT-qPCR
dT20	TTTTTTTTTTTTTTTTTTTT	dT20 primer for reverse transcription
NC988	CATGCATTGCGTCTCAAACCT	OGT exon 3 forward primer
NC1769	TTCAGAGAGTCTGCATGGGT	OGT exon 8 reverse primer
NC4588	CACAAGATCCTCATCGACAGATA	SFSWAP forward primer for RT-qPCR
NC4589	CTCCTCTTCAGACAGCTGATAAT	SFSWAP reverse primer for RT-qPCR
NC1224	ACCCAGCACAATGAAGATCA	β-actin forward primer for RT-qPCR
NC1225	CTCGTCATACTCCTGCTTGC	β-actin reverse primer for RT-qPCR
NC3739	CTTCGAATTCTGCAGTCGACGGTA CCATGGTGAGCAAGGGCGAGGA	BamHI site containing reverse primer for OGT reporter cloning
NC3482	GGGAAAGAAAACATCAAGGG	Acc65I site containing forward primer for OGT reporter cloning
NC2085	CTGAGTGAGCTGCACTGTGA	Forward primer used in OGT reporter cloning; introduces BamHI site
NC3851	GATTATGATCTAGAGTCGCGGCC GCTTTAGTGATACTTGTGGGCCA	Reverse primer used in OGT reporter cloning; introduces XbaI site
NC3378	TAAACGGCCACAAGTTCAGC	Forward primer used for OGT reporter validation; binds GFP ORF
NC2094	CACCAGCCACCACTTTCTGA	Reverse primer used for OGT reporter validation
NC985	ACACAGCCAAGATTACTCCAAG	OGT exon 5 reverse primer used for reverse transcription
NC2909	ACCACATGAAGCAGCACGAC	Forward primer used to generate GFP probe for northern blot analysis
NC4001	TAATACGACTCACTATAGGGATCT TGAAGTTCACCTTGATG	Reverse primer used to generate GFP probe for northern blot analysis
NC2018	CAGTGTAAATCACGGAATATC	Forward primer used to generate OGT probe for northern blot analysis
NC1248	TAATACGACTCACTATAGGGAAGG ATCGCAAGACAACATCT	Reverse primer used to generate OGT probe for northern blot analysis

Fig. 1

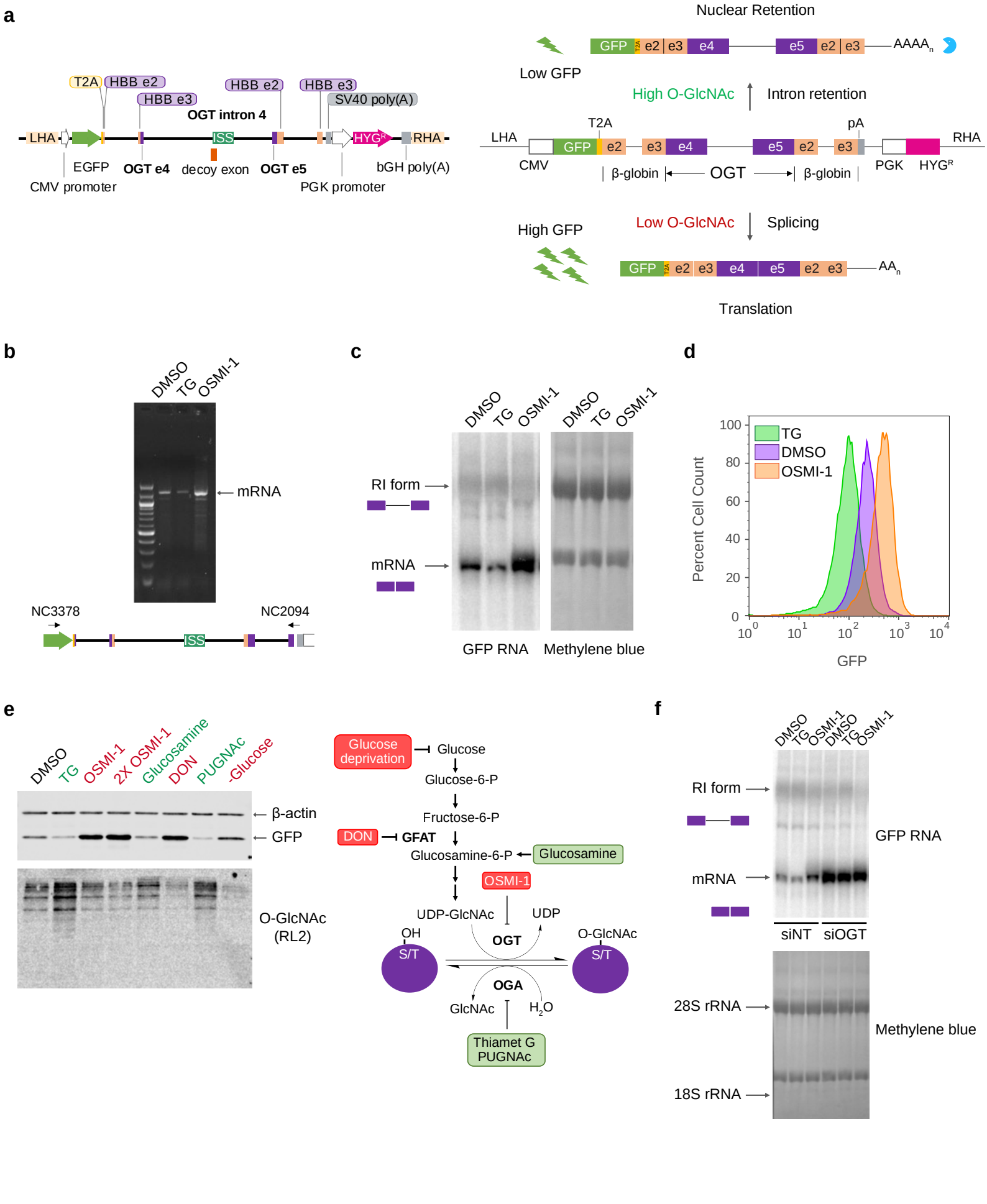

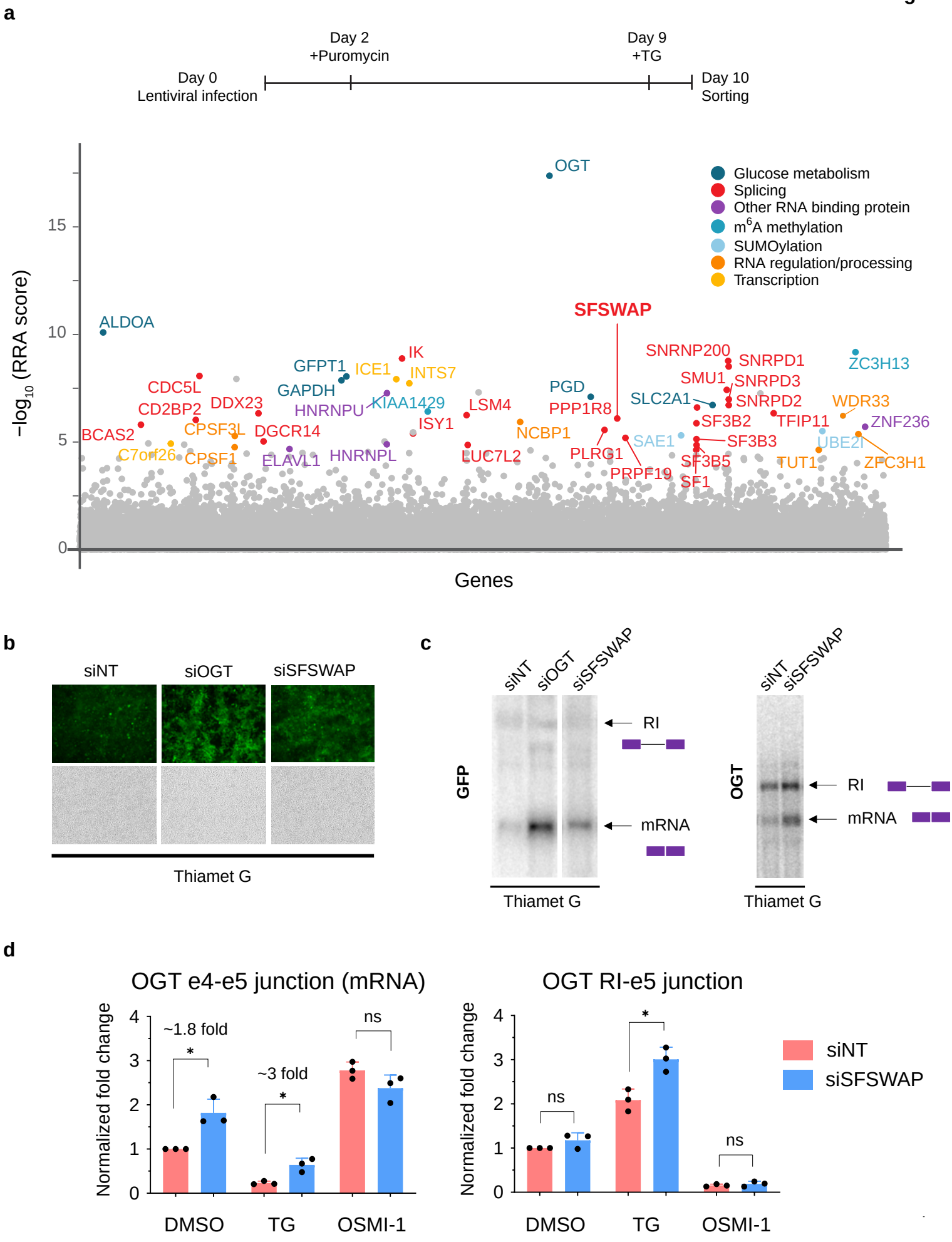

Fig. 3

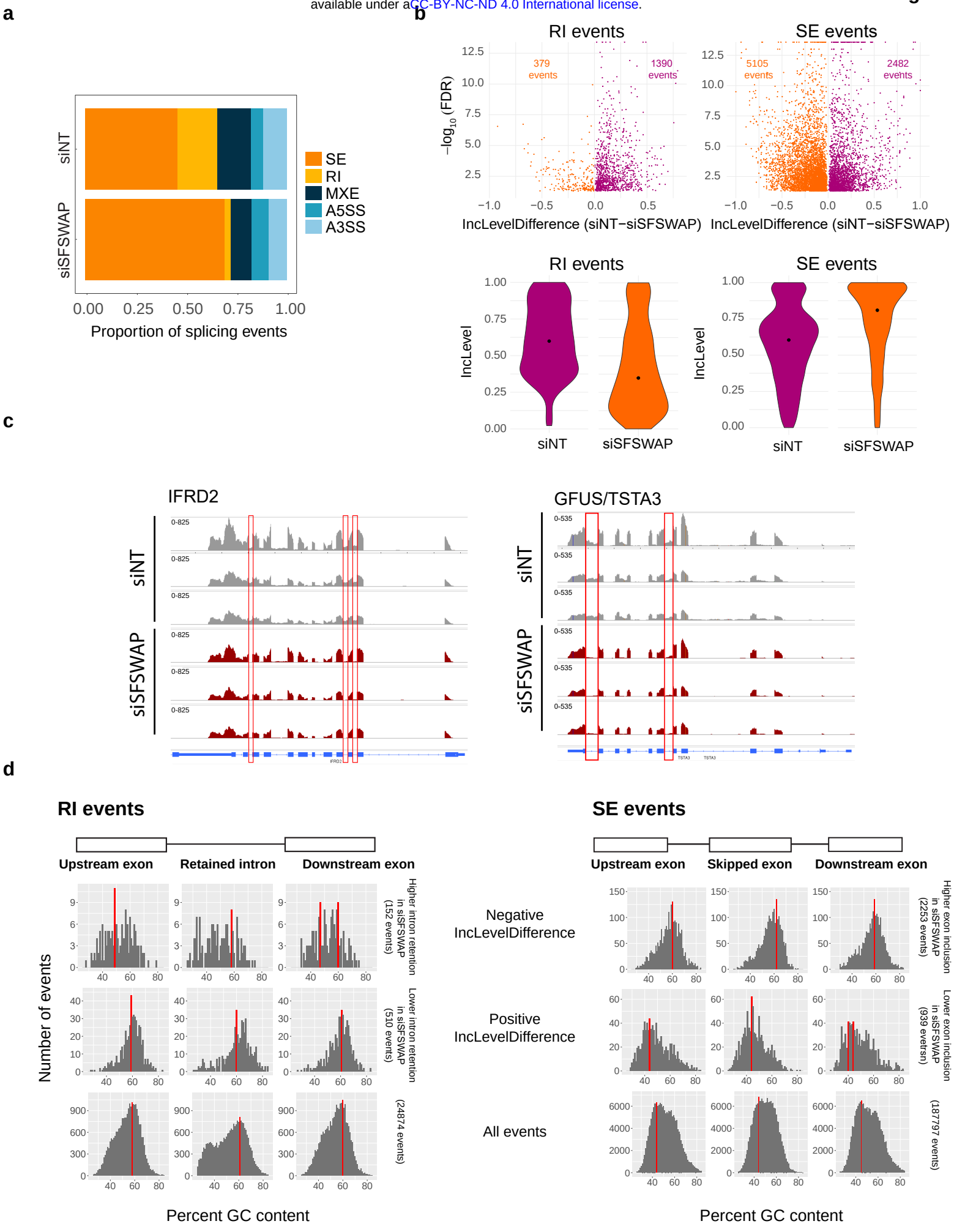

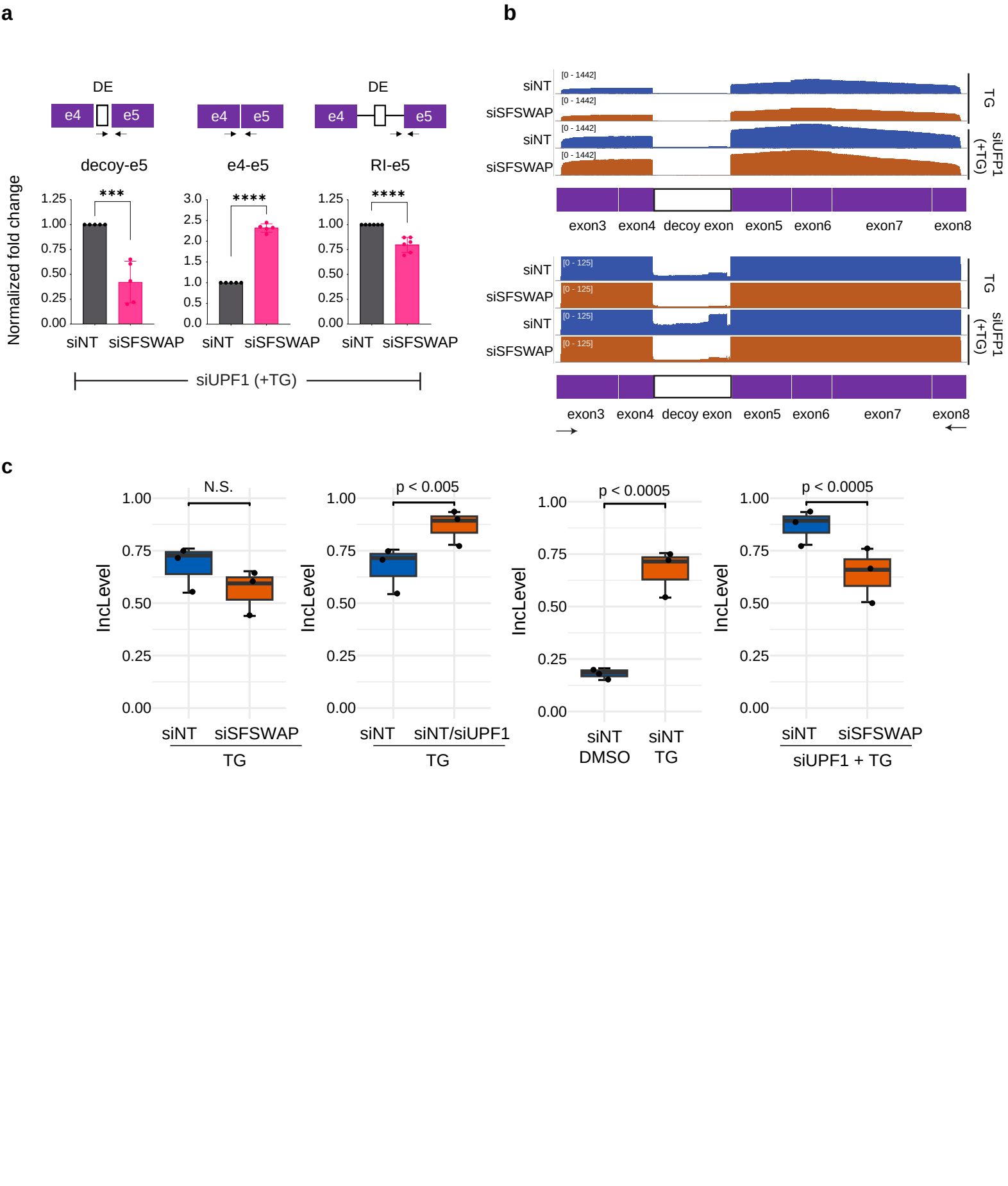

Fig. 5

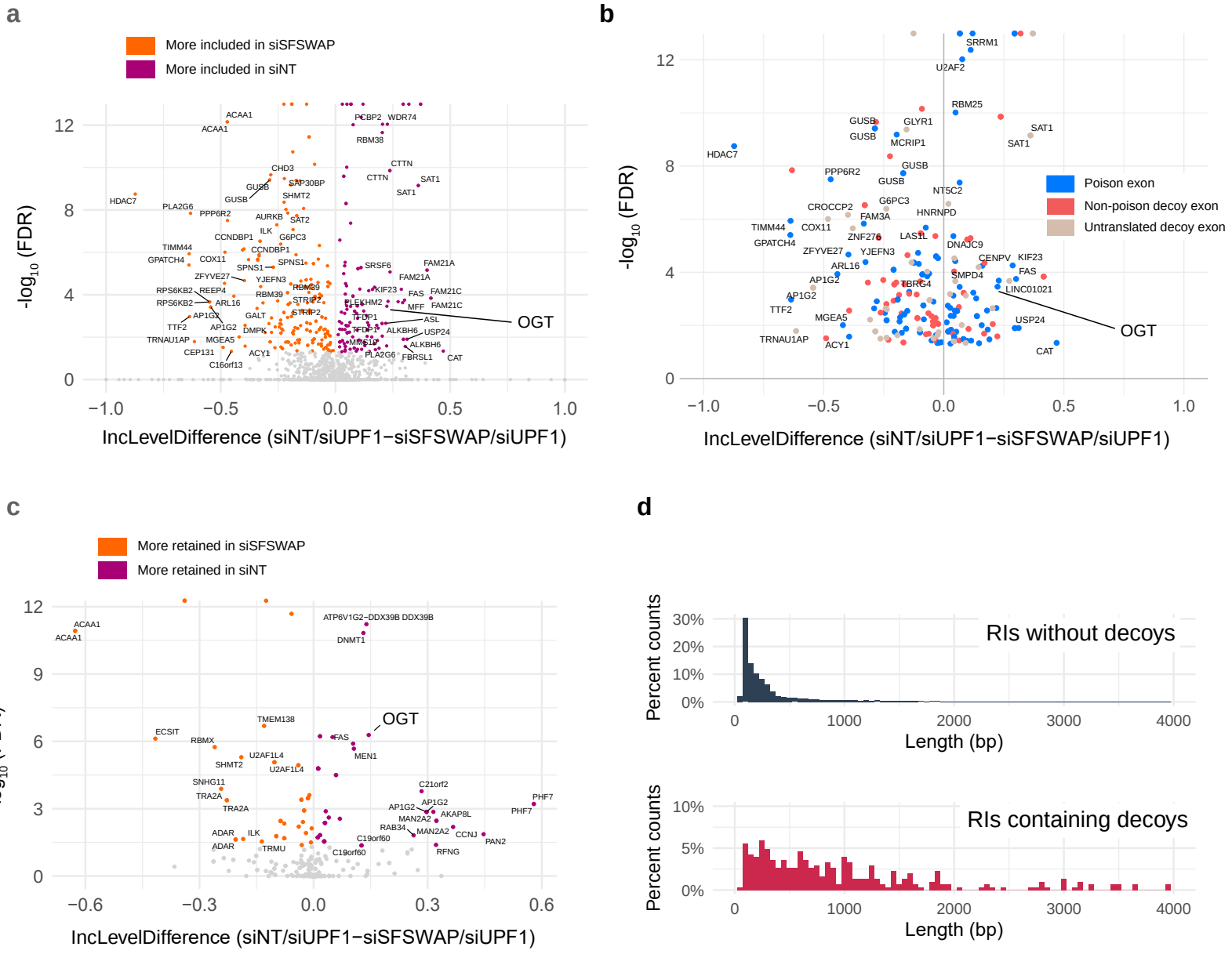

Fig. 6

Wildtype

Retained introns

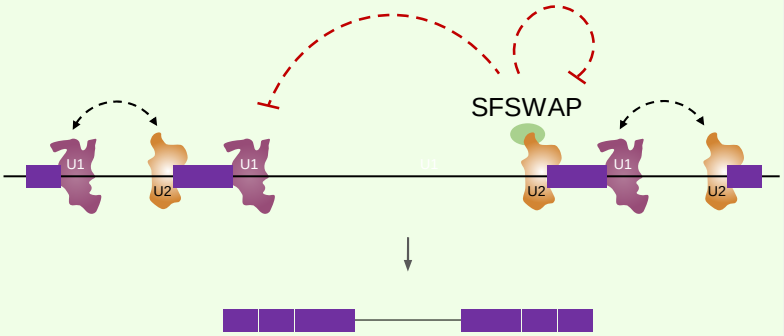

Intron retention

Skipped exons

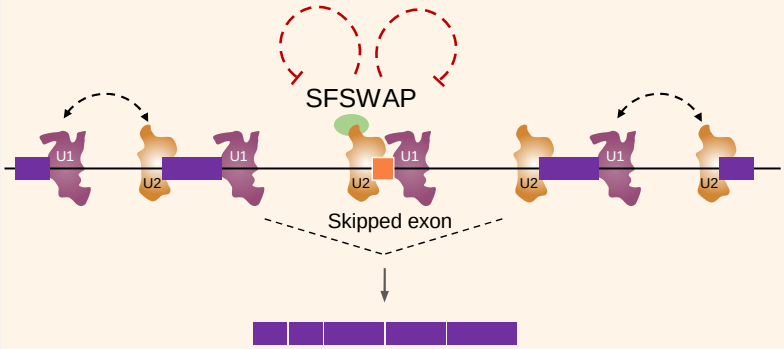

Exon skipping

Decoy-containing retained introns (OGT)

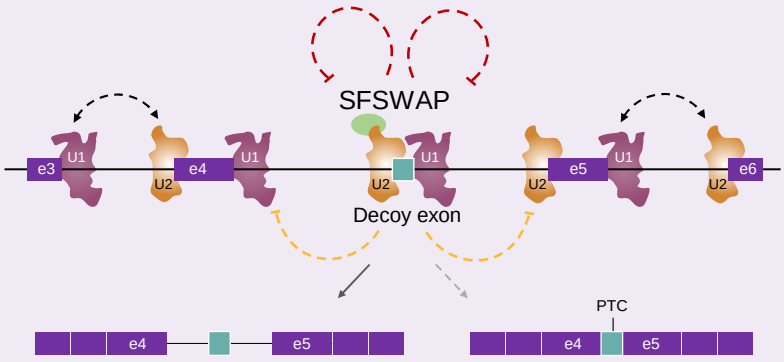

Intron retention

Non-productive splicing

SFSWAP knockout

Retained introns

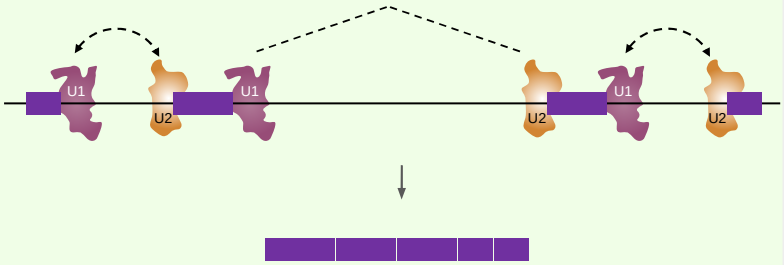

Productive splicing

Skipped exons

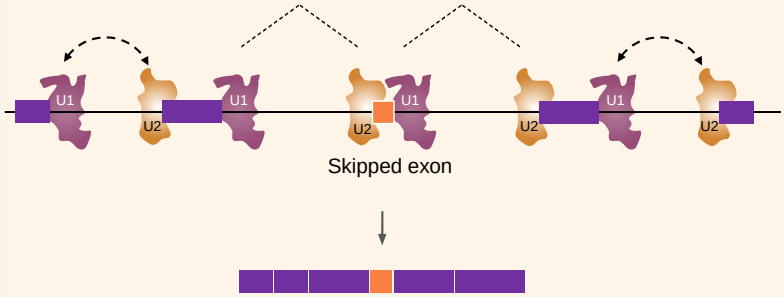

Exon inclusion

Decoy-containing retained introns (OGT)

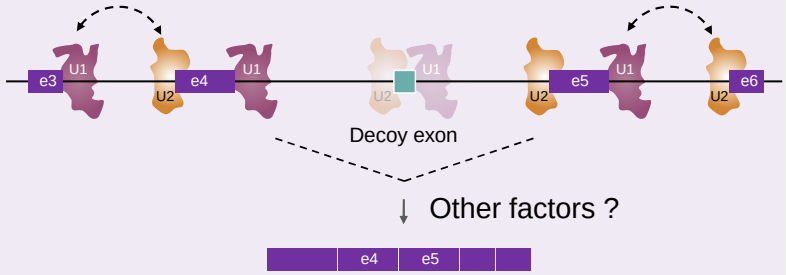

Productive splicing

Fig. S1

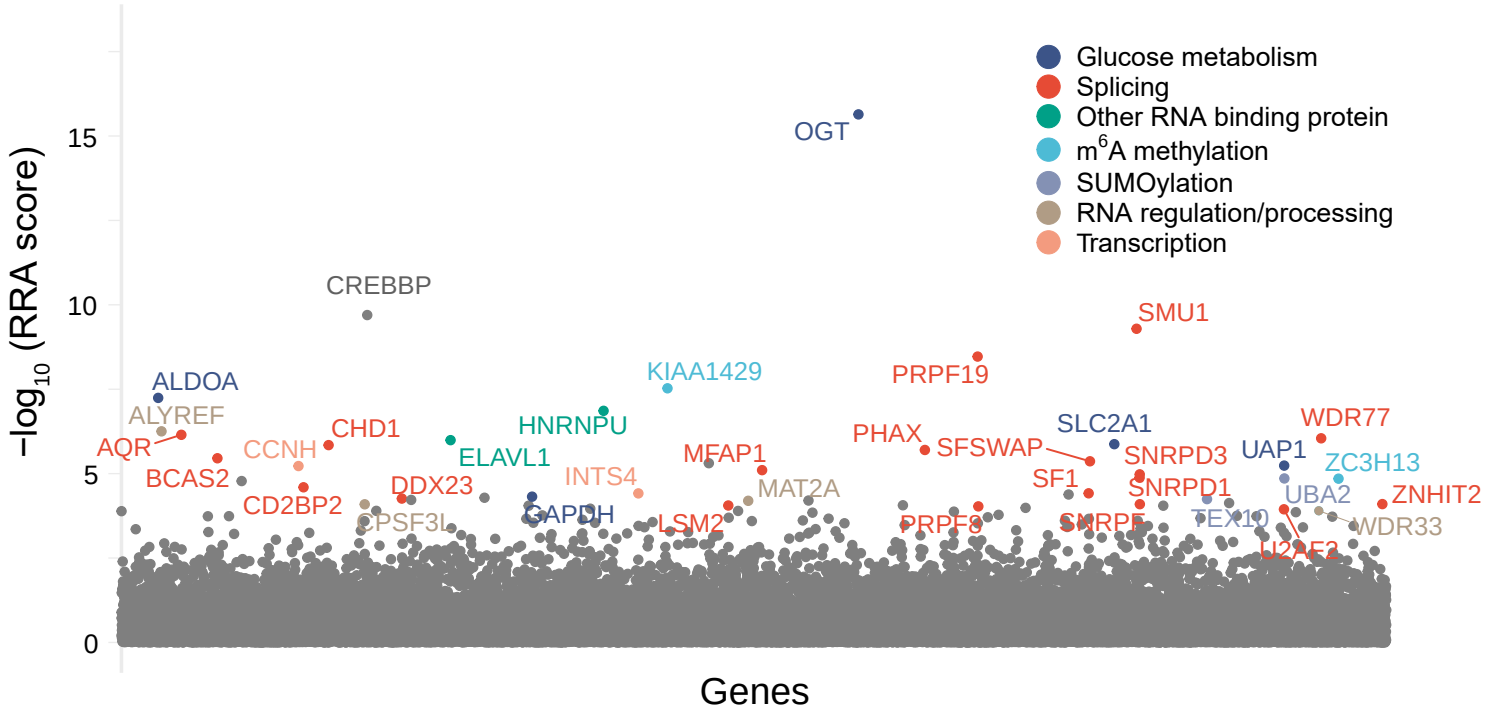

Fig. S2

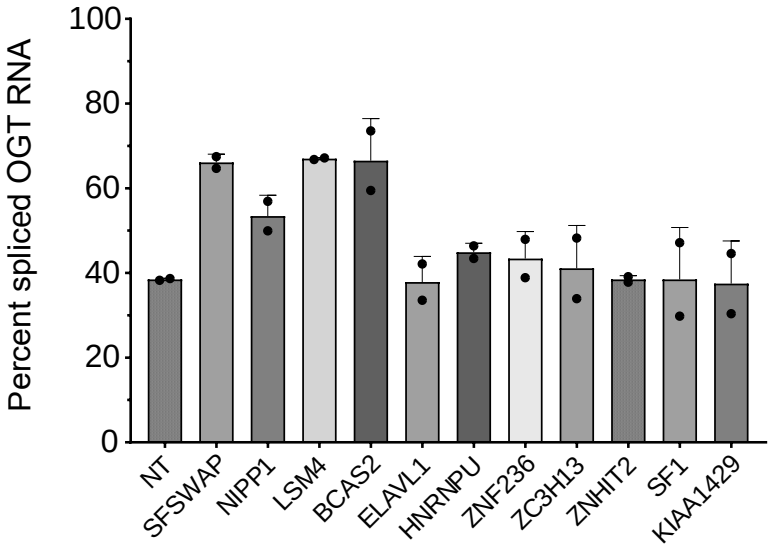

Fig. S3

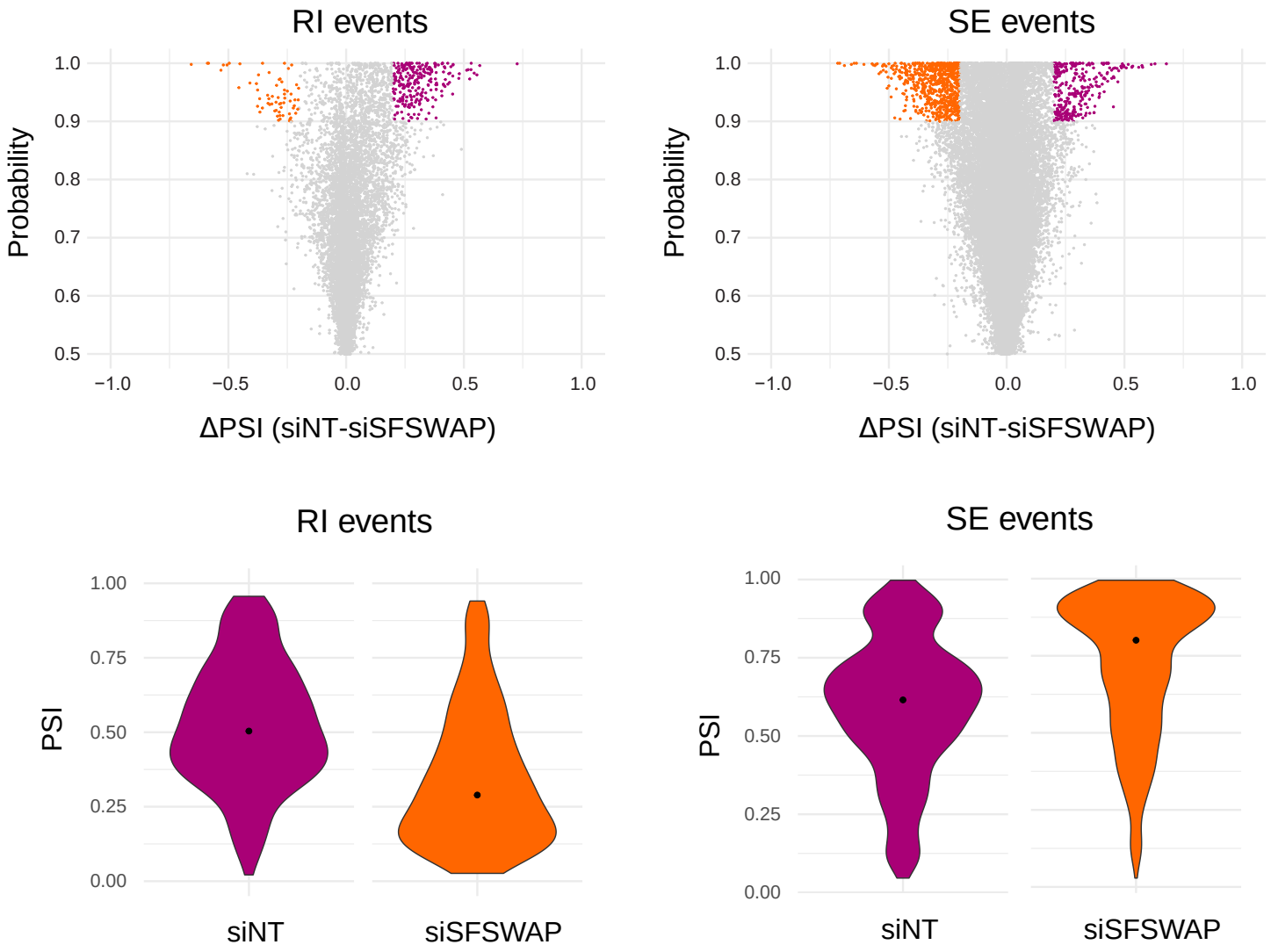

Fig. S4

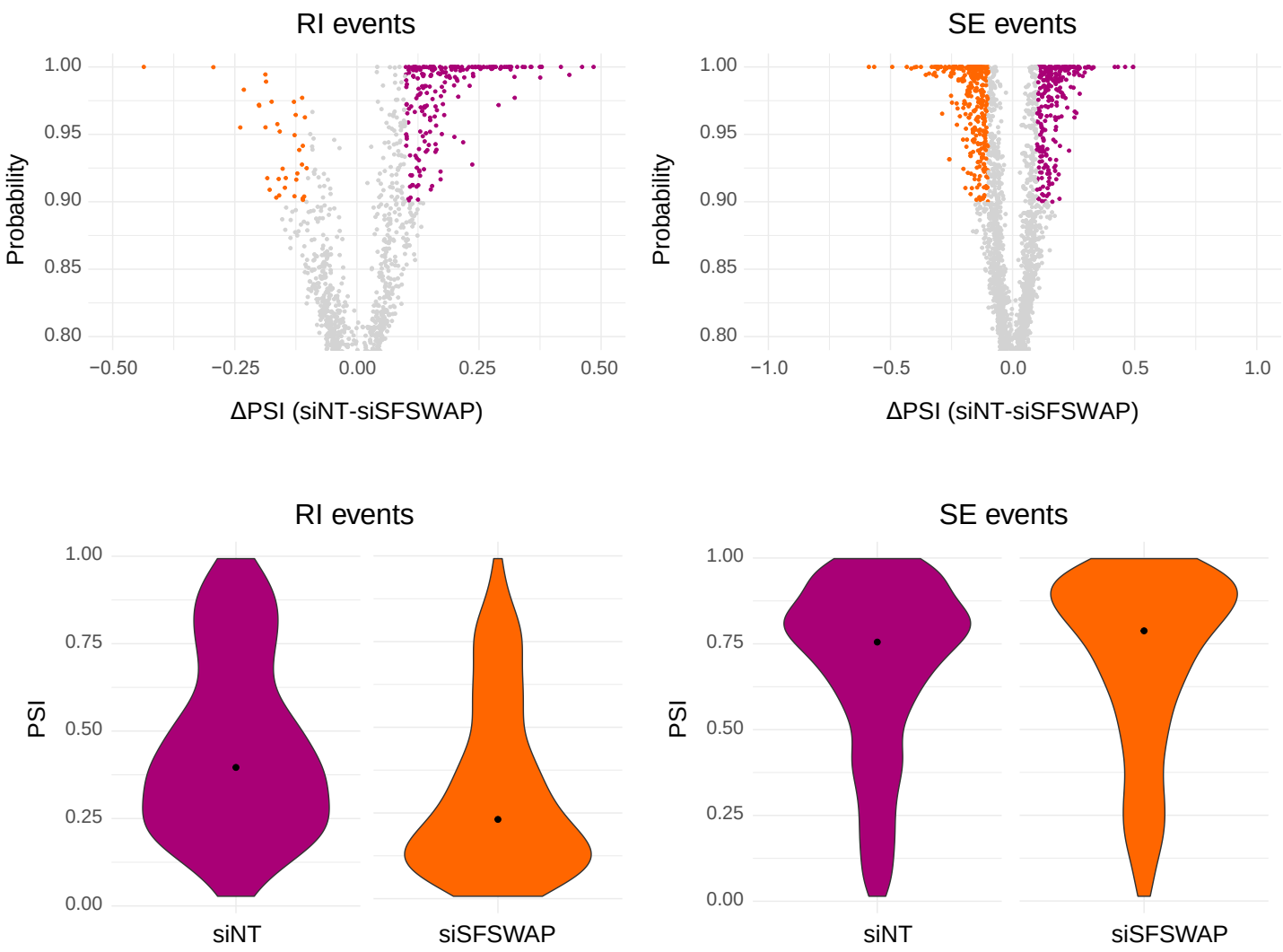

Fig. S5

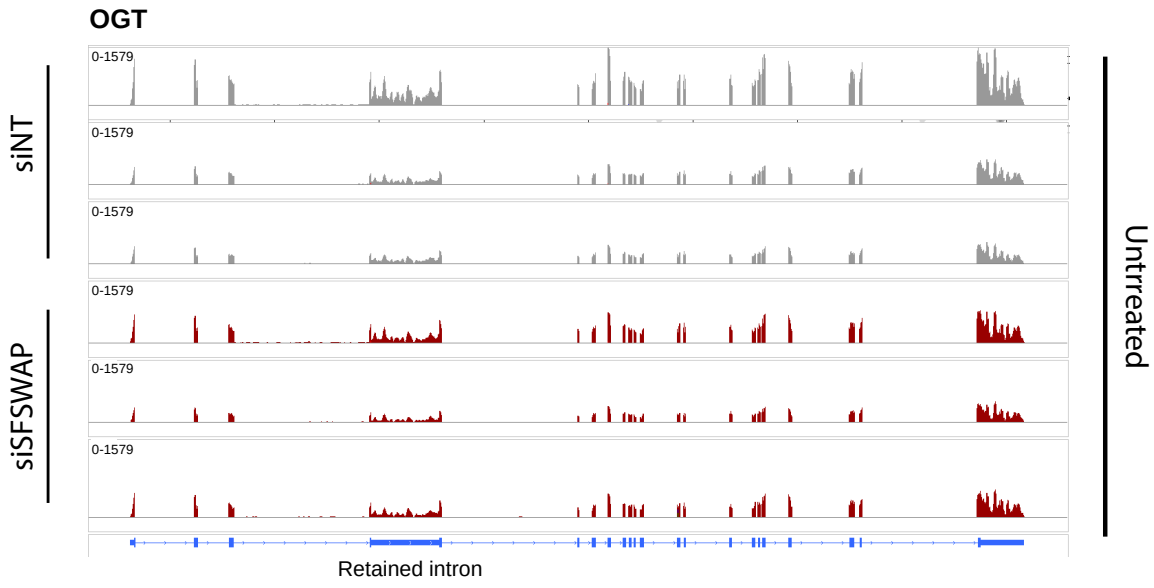

Fig. S6

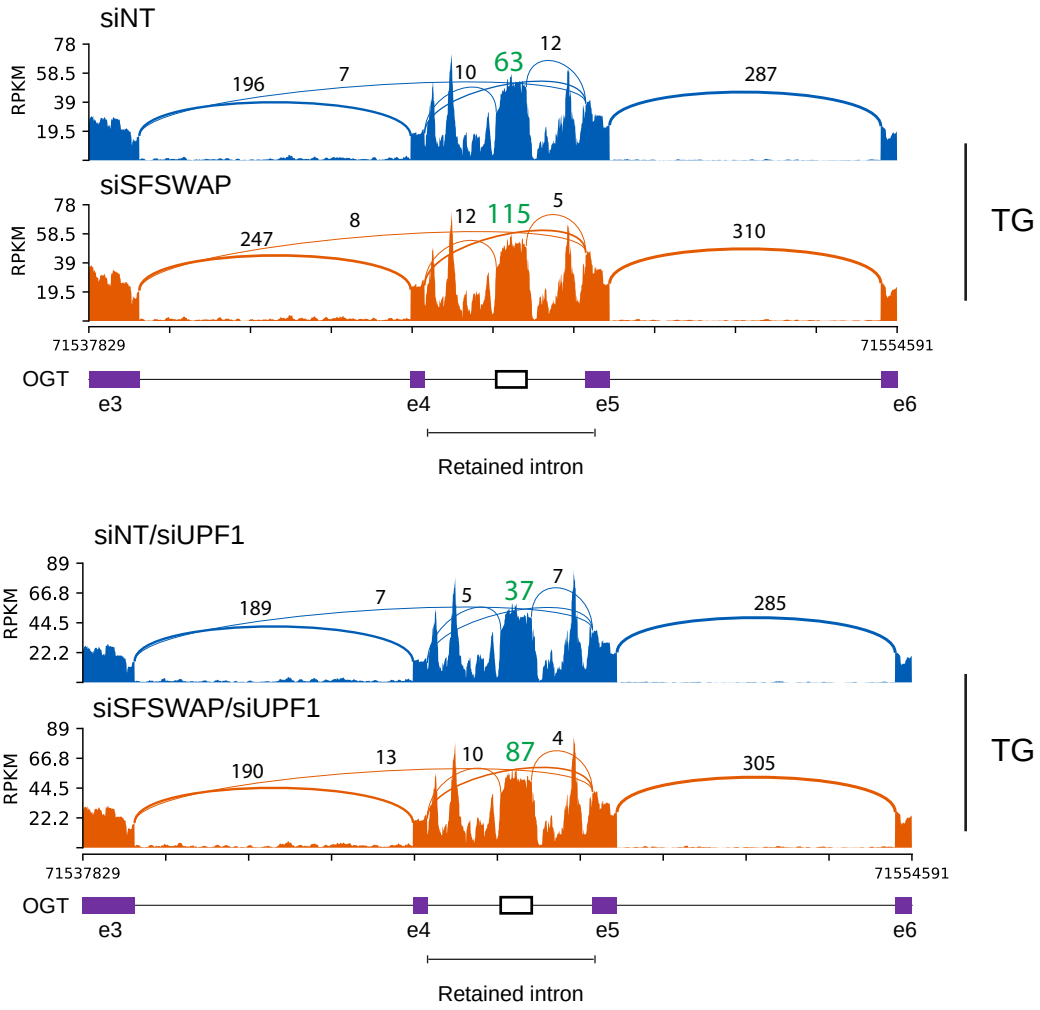

Fig. S7

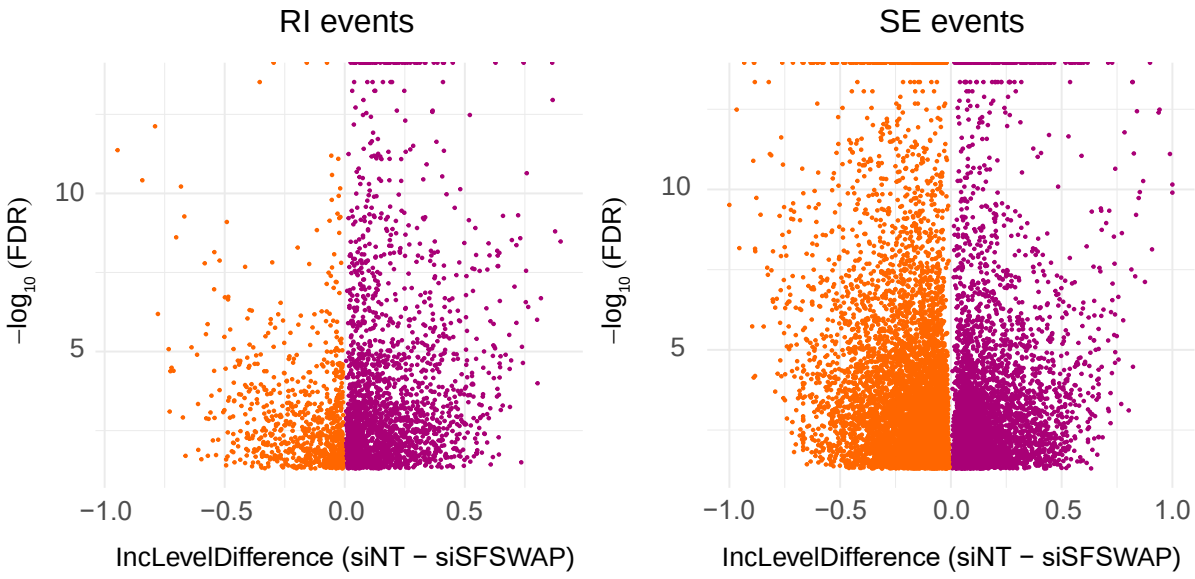

Fig. S8

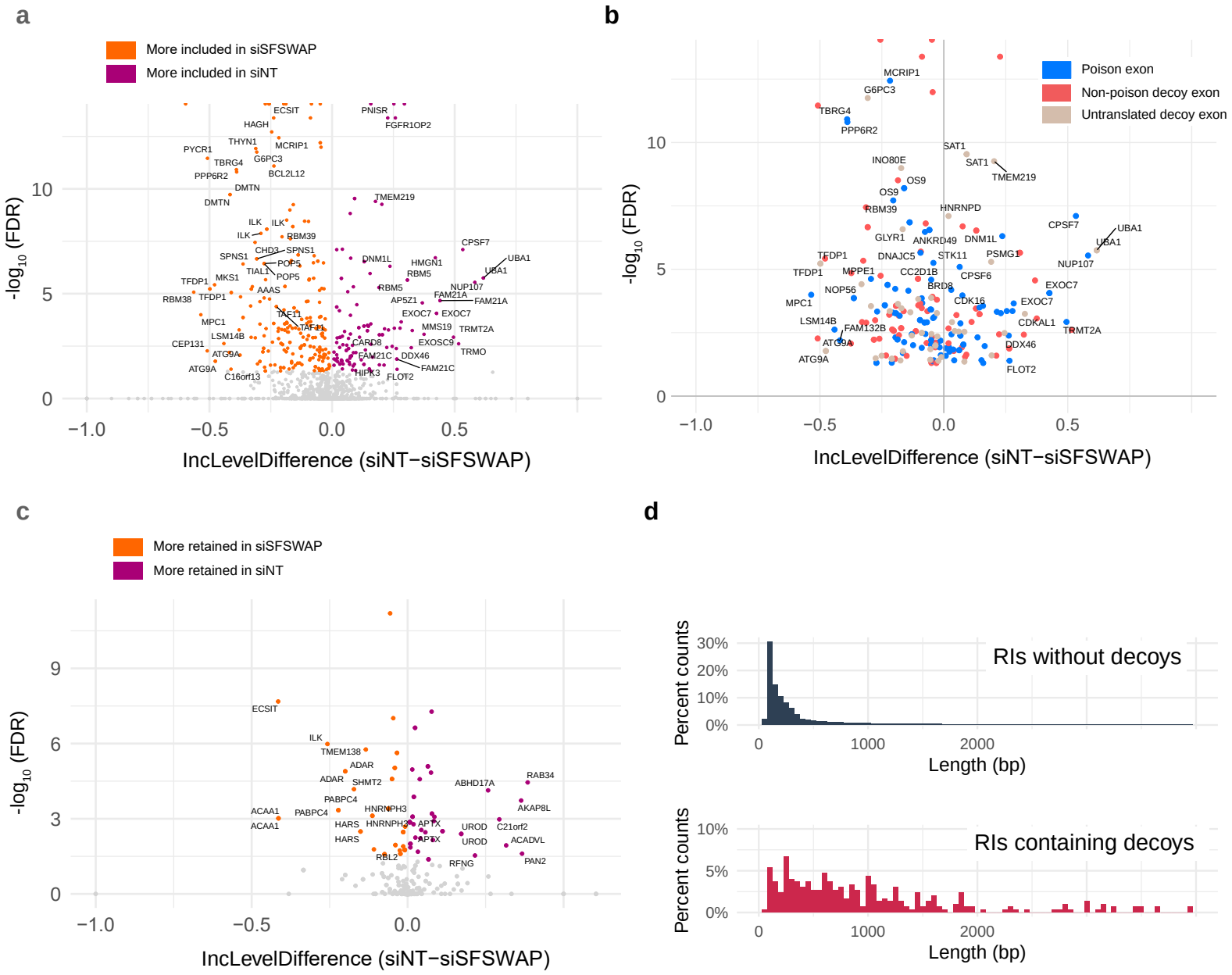

Fig. S9

Retained intron events

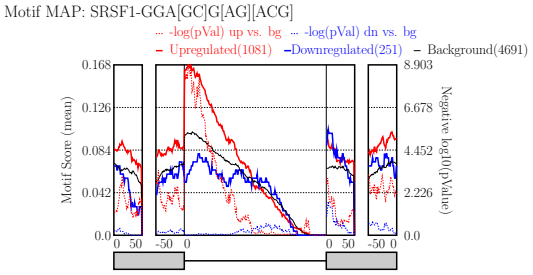

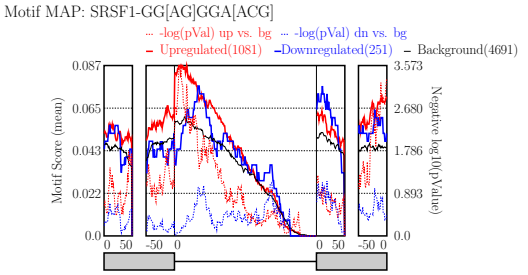

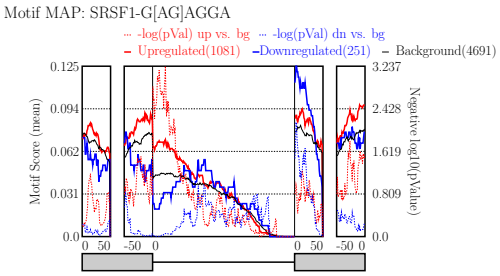

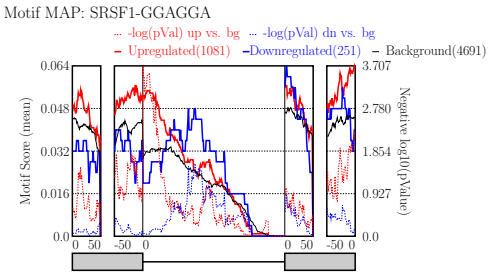

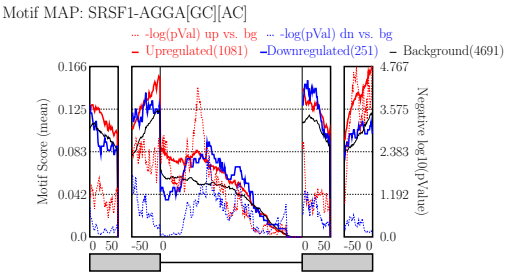

Skipped exon events

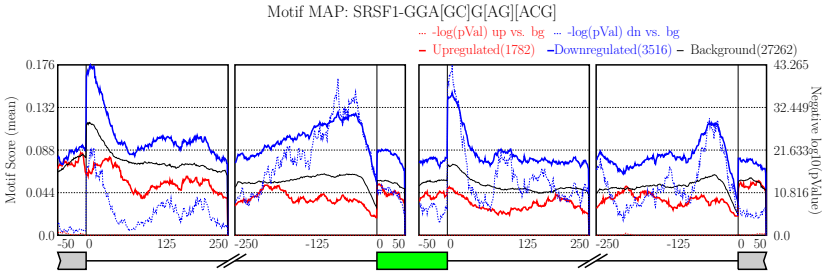

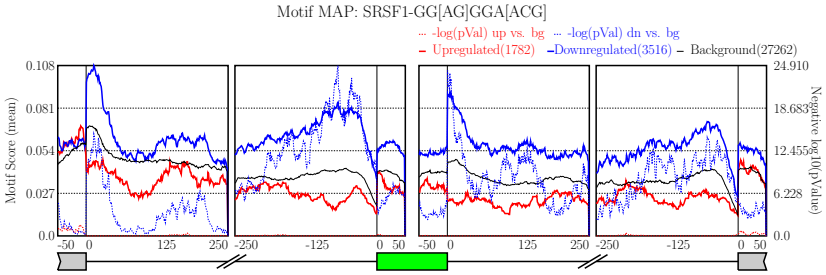

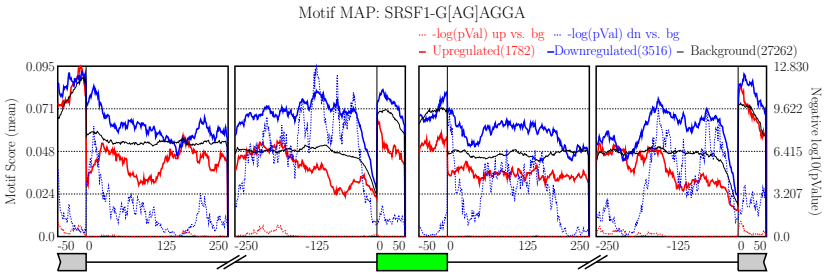

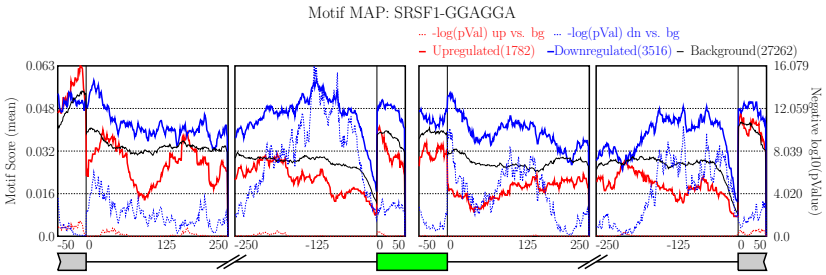

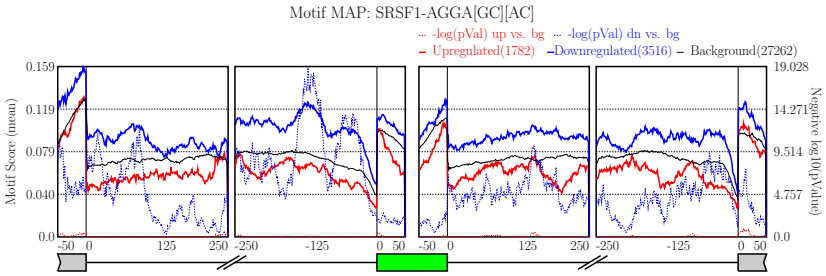

Fig. S10

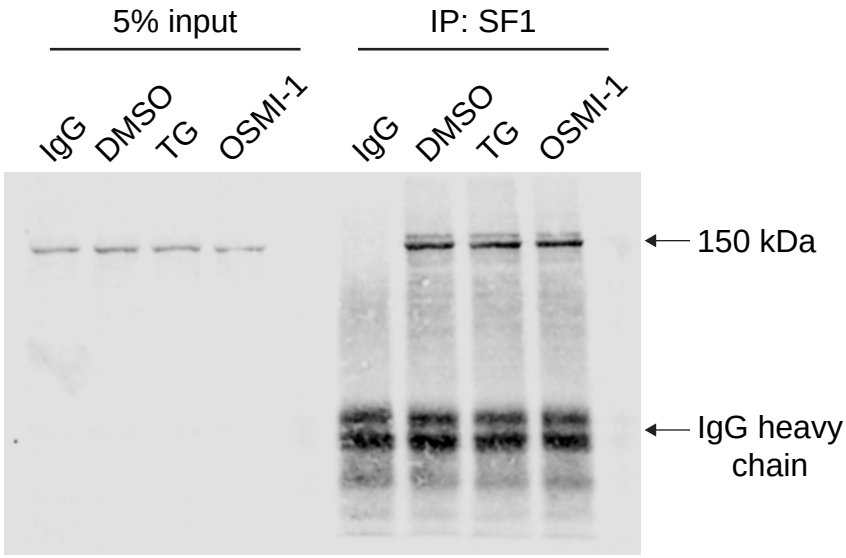

α-SFSWAP

Fig. S11

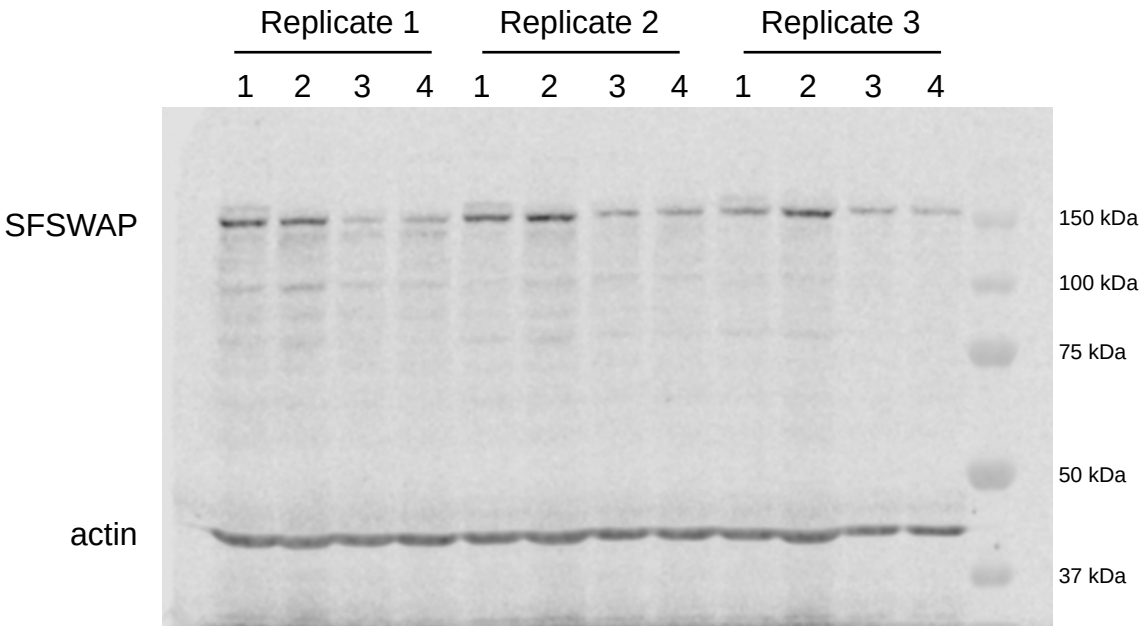

1. siNT
2. siSFSWAP (siRNA #1)
3. siSFSWAP (siRNA #2)
4. siSFSWAP (siRNA #1+2) (used for RNA-seq experiments)

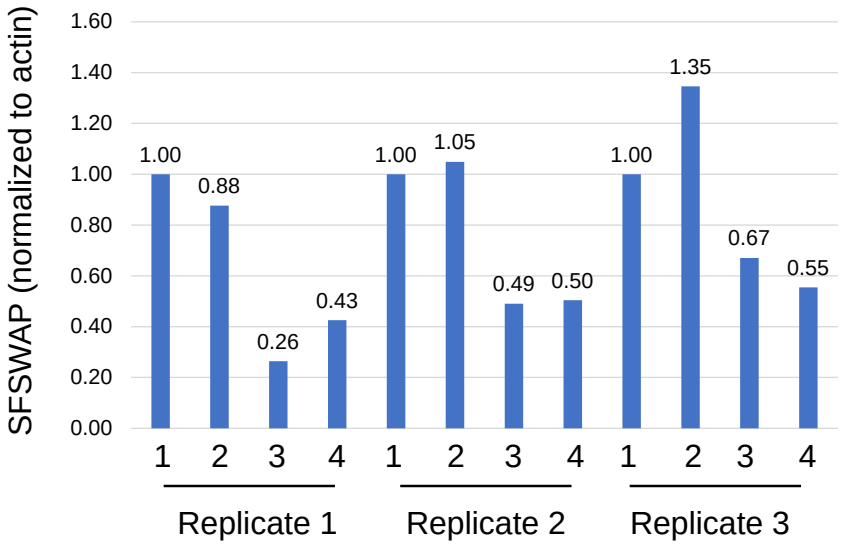

Fig. S12

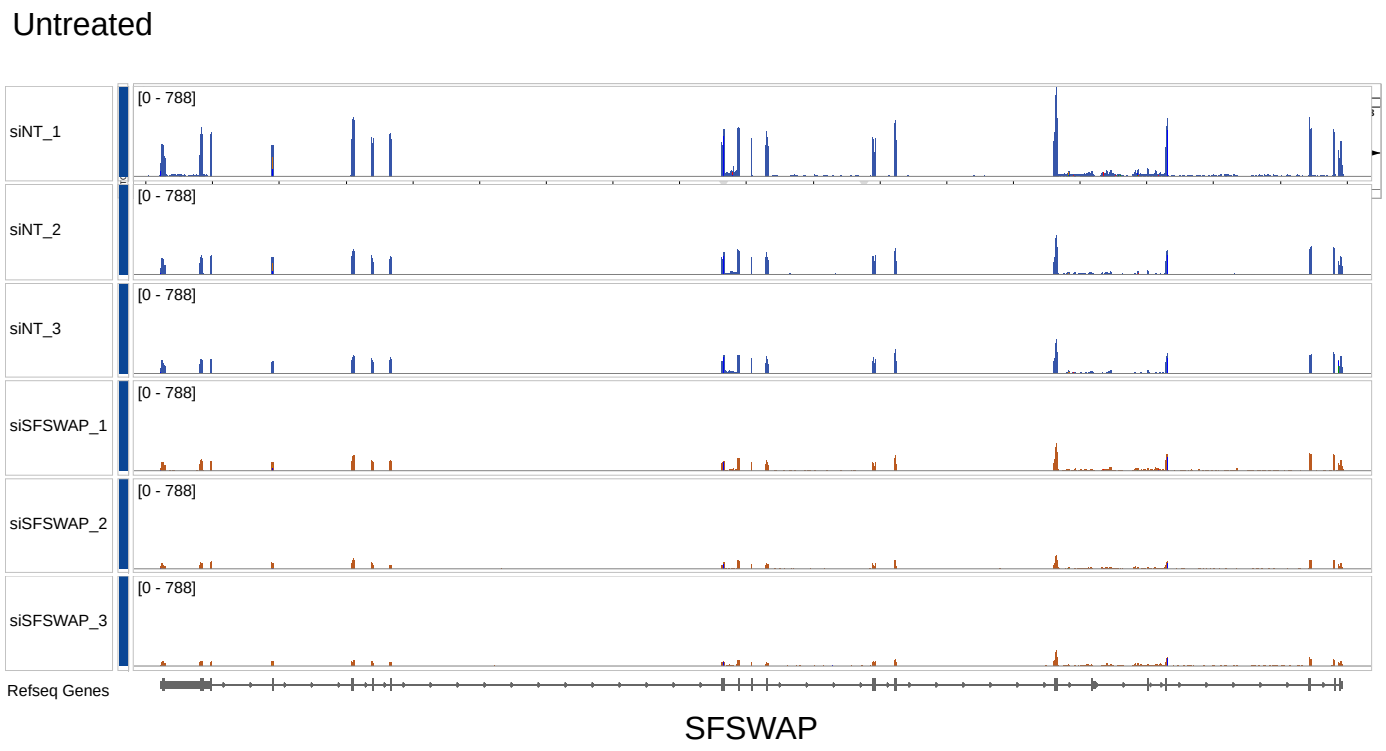

Fig. S13

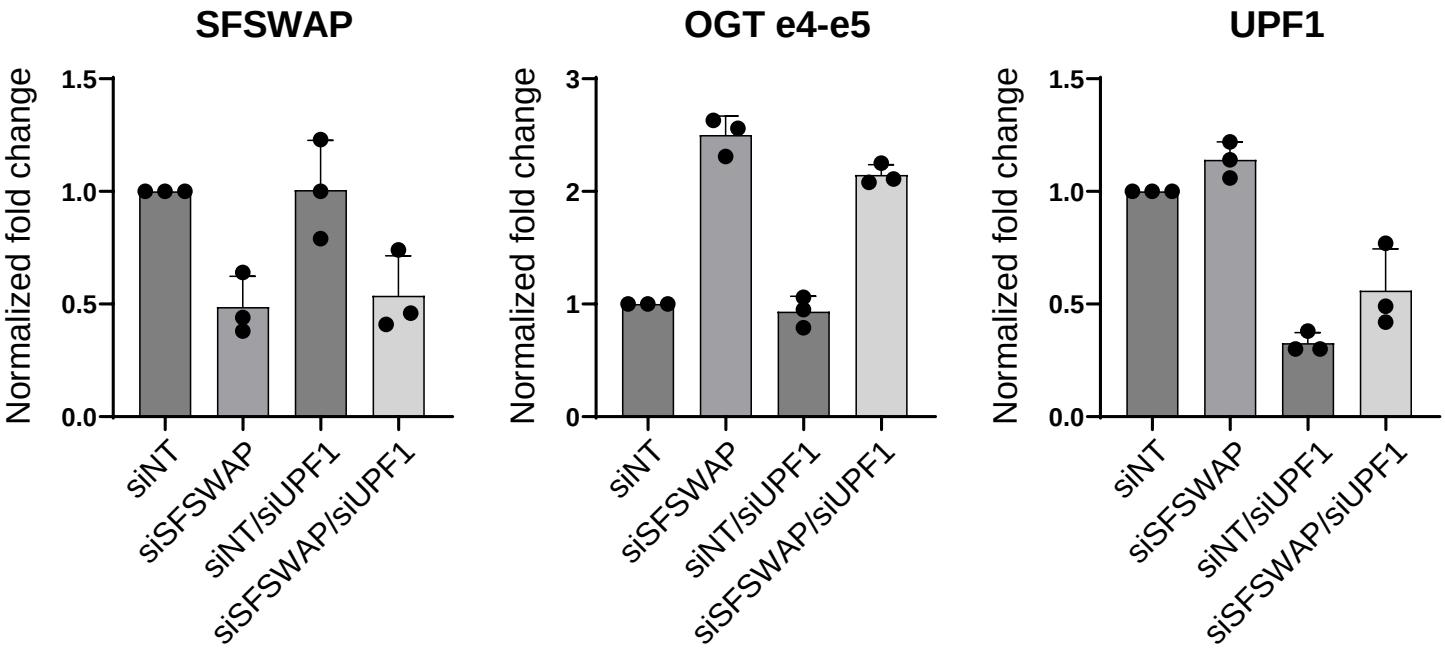

Fig. S14

TG

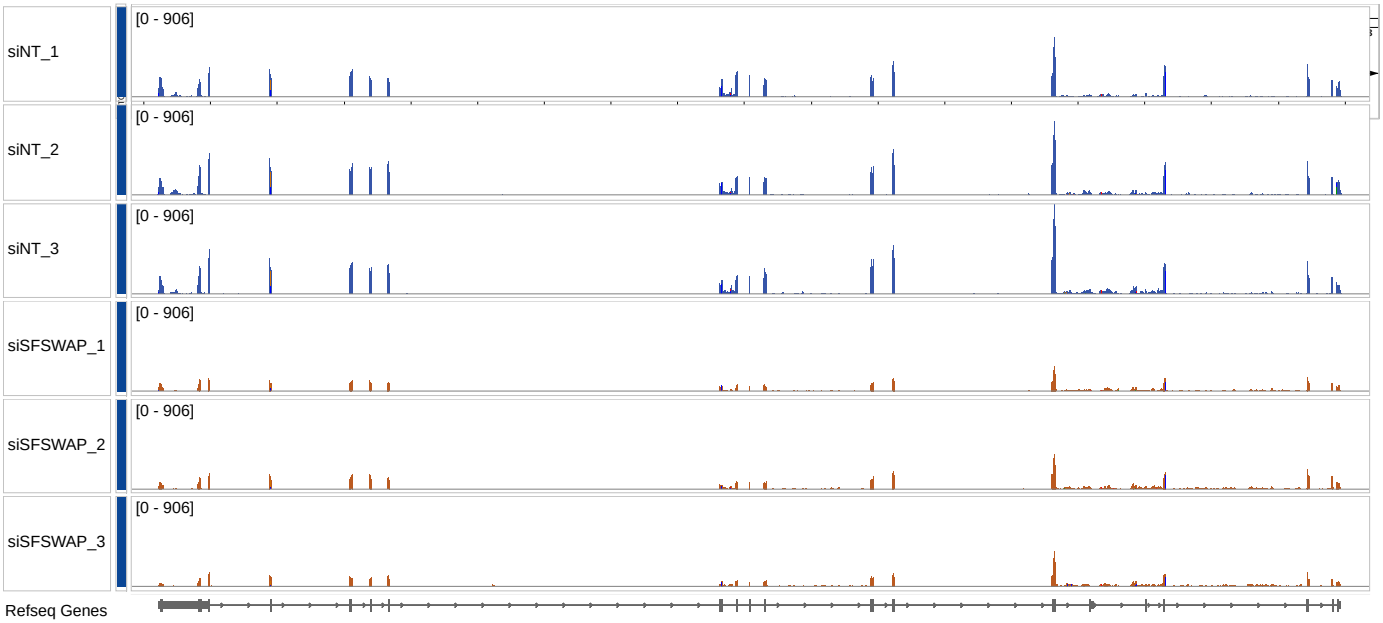

siUPF1 (+TG)